This article was downloaded by: [Auckland University of Technology]
On: 09 March 2015, At: 15:24
Publisher: Taylor & Francis
Informa Ltd Registered in England and Wales Registered Number: 1072954 Registered office: Mortimer House, 37-41 Mortimer Street, London W1T 3JH, UK

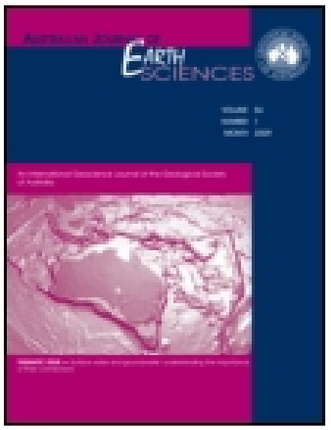

Australian Journal of Earth Sciences: An International Geoscience Journal of the Geological Society of Australia
Publication details, including instructions for authors and subscription information:
http://www.tandfonline.com/loi/taje20

Middle and Late Ordovician magmatic evolution of the Macquarie Arc, Lachlan Orogen, New South Wales

A. J. Crawford [a], S. Meffre [a], R. J. Squire [b], L. M. Barron [c] & T. J. Falloon [d]

[a] ARC Centre of Excellence in Ore Deposits, School of Earth Sciences, University of Tasmania, Private Bag 79, Hobart, Tas., 7001, Australia

[b] School of Geosciences, Monash University, Vic., 3800, Australia

[c] Geological Survey of New South Wales, Department of Primary Industries, PO Box 344, Hunter Regional Mail Centre, NSW, 2310, Australia

[d] School of Earth Sciences, University of Tasmania, Private Bag 79, Hobart, Tas, 7001, Australia

Published online: 06 Oct 2011.

To cite this article: A. J. Crawford, S. Meffre, R. J. Squire, L. M. Barron & T. J. Falloon (2007) Middle and Late Ordovician magmatic evolution of the Macquarie Arc, Lachlan Orogen, New South Wales, Australian Journal of Earth Sciences: An International Geoscience Journal of the Geological Society of Australia, 54:2-3, 181-214, DOI: 10.1080/08120090701227471

To link to this article: http://dx.doi.org/10.1080/08120090701227471

PLEASE SCROLL DOWN FOR ARTICLE

Taylor & Francis makes every effort to ensure the accuracy of all the information (the "Content") contained in the publications on our platform. However, Taylor & Francis, our agents, and our licensors make no representations or warranties whatsoever as to the accuracy, completeness, or suitability for any purpose of the Content. Any opinions and views expressed in this publication are the opinions and views of the authors, and are not the views of or endorsed by Taylor & Francis. The accuracy of the Content should not be relied upon and should be independently verified with primary sources of information. Taylor and Francis shall not be liable for any losses, actions, claims, proceedings, demands, costs, expenses, damages, and other liabilities whatsoever or howsoever caused arising directly or indirectly in connection with, in relation to or arising out of the use of the Content.

This article may be used for research, teaching, and private study purposes. Any substantial or systematic reproduction, redistribution, reselling, loan, sub-licensing, systematic supply, or distribution in any form to anyone is expressly forbidden. Terms & Conditions of access and use can be found at http://www.tandfonline.com/page/terms-and-conditions

Australian Journal of Earth Sciences (2007) **54**, (181–214)

Middle and Late Ordovician magmatic evolution of the Macquarie Arc, Lachlan Orogen, New South Wales

A. J. CRAWFORD[1]*, S. MEFFRE[1], R. J. SQUIRE[2], L. M. BARRON[3†] AND T. J. FALLOON[4]

[1]*ARC Centre of Excellence in Ore Deposits, School of Earth Sciences, University of Tasmania, Private Bag 79, Hobart, Tas. 7001, Australia.*
[2]*School of Geosciences, Monash University, Vic. 3800, Australia.*
[3]*Geological Survey of New South Wales, Department of Primary Industries, PO Box 344, Hunter Regional Mail Centre, NSW 2310, Australia.*
[4]*School of Earth Sciences, University of Tasmania, Private Bag 79, Hobart, Tas. 7001, Australia.*

Downloaded by [Auckland University of Technology] at 15:24 09 March 2015

Early Ordovician (Phase 1) magmatism in the Macquarie Arc was followed by a magmatic hiatus of ~9 million years, between late Bendigonian and early Darriwilian (i.e. between *ca* 475 and *ca* 466 Ma). Resumption of magmatism in the Middle Ordovician produced Phase 2 rocks, recorded by three major rock suites: (i) medium-K calc-alkaline lavas in the Cargo block (Molong Volcanic Belt) have primitive ε_{Nd} values (+6.9 to +7.8) and volcanic facies suggesting eruption in an intra-oceanic arc stratovolcano; lavas in the fault-bounded Parkes Volcanics in the Junee–Narromine Volcanic Belt are compositionally identical to those in the Cargo block, suggesting that similar Phase 2 Middle Ordovician arc-type lavas may underlie the Cowra Trough; (ii) medium- to high-K dioritic to monzodioritic intrusions in the Narromine and Cowal Igneous Complexes of the Junee–Narromine Volcanic Belt have ages that cluster in the 470–460 Ma interval, and intrude presumed Phase 1 lavas and volcaniclastics; and (iii) in all three main volcanic belts, Middle Ordovician lavas range from medium-K to dominantly high-K calc-alkaline compositions with a clear trend to shoshonitic compositions late in the Phase 2 magmatic episode. Phase 2 units in the Molong Volcanic Belt (lower Blayney, Byng and lower Fairbridge Volcanics) and Rockley–Gulgong Volcanic Belt (Rockley and lower Sofala Volcanics) are dominated by significantly more unfractionated high-MgO lava compositions than contemporaneous lavas in the Cargo block or Junee–Narromine Volcanic Belt, suggesting that rifting of the arc had occurred by this time, and that the main extensional zone lay along the eastern side of the Macquarie Arc. Identical compositions of unusual shoshonitic ultramafic lavas in the Byng Volcanics of the Molong Volcanic Belt and the Rockley Volcanics of the Rockley–Gulgong Volcanic Belt provide strong evidence that these volcanic belts were once contiguous and were disrupted during Silurian–Devonian opening of the Hill End Trough. Phase 3 magmatism in the Macquarie Arc is represented by a widespread but relatively small volume magmatic event, dominated by shallow intrusive rocks of the Copper Hill Suite, emplaced in the Eastonian–Bolindian, between 456 and 441 Ma. These distinctive porphyritic dacites and associated holocrystalline diorites and granodiorites show medium-K calc-alkaline compositions, and their emplacement was intimately linked to an episode of regional uplift, erosion and limestone deposition in the Junee–Narromine Volcanic Belt and western Molong Volcanic Belt. Phase 4 magmatism extended from late Eastonian or Bolindian until Early Silurian time, and was dominated by relatively evolved (compared with Phase 2 lavas) shoshonitic lavas until the end of the Bolindian and porphyries in the Early Silurian. Collision-related shut-down of the arc, and initiation of arc extension and dismemberment, occurred around 438 Ma in the latest Ordovician. Post-arc magmatism during the Early Silurian is represented by high-Th, high-Nb lavas of the shoshonitic Nash Hill Volcanics in the Junee–Narromine Volcanic Belt, and Alaskan-type zoned ultramafic intrusions of the Fifield complexes farther west. The latter were emplaced through deformed Ordovician turbidites of the Girilambone Group, and their radiogenic isotope signatures show significant crustal involvement.

KEY WORDS: Lachlan Orogen, Macquarie Arc, magmatism, Ordovician, shoshonites.

INTRODUCTION

The Ordovician to Early Silurian Macquarie Arc is a key component of the Eastern Subprovince of the Lachlan Orogen of southeastern Australia. Magmatism forming the Macquarie Arc commenced before 484 Ma in the Early Ordovician (Glen *et al.* 2007a; Percival & Glen 2007). However, most igneous rocks in the three

*Corresponding author: tony.crawford@utas.edu.au
†Present address: 7 Fairview Place, St Ives, NSW 2075, Australia.

ISSN 0812-0099 print/ISSN 1440-0952 online © 2007 Geological Society of Australia
DOI: 10.1080/08120090701227471

Downloaded by [Auckland University of Technology] at 15:24 09 March 2015

volcanic belts that make up the now-dismembered arc formed in the Middle to Late Ordovician and preserve a record of the tectono-magmatic development of this arc until its demise around 438 Ma in the earliest Silurian. Research during the New South Wales Ordovician SPIRT Project showed that the Macquarie Arc formed during four separate phases of arc-type magmatism separated by either hiatuses in volcanism or periods of limestone deposition. The earliest volcanic phase, Phase 1, occurred in the Early Ordovician and is documented in an accompanying paper (Glen *et al.* 2007a).

This paper describes the products of Phases 2–4 based on a comprehensive petrological–geochemical study of Middle and Late Ordovician and Early Silurian igneous rocks in the three major volcanic belts, namely the Junee–Narromine Volcanic Belt in the west, the central Molong Volcanic Belt, and the Rockley–Gulgong Volcanic Belt in the east. Also briefly described are those rocks exposed in the Kiandra Belt in the Snowy Mountains (Figure 1). Based on carefully selected least-altered rocks, the major aims of the study were to: (i) document temporal changes in the geochemical affinities of the magmatic rocks and evaluate their implications for the tectonic development of the arc; and (ii) compare the chemical lithostratigraphy of each of these belts, in order to establish whether they originally formed a single arc that subsequently was dismembered during Silurian deformation (Glen *et al.* 1998), or were separate belts with distinct histories.

Biostratigraphic and radiometric dating underpinning the lithostratigraphy in each volcanic belt is presented in detail in Percival and Glen (2007). A compendium of all the analytical data referred to herein is given in a GIS compilation (Glen et al. 2004b), and tables of representative data are provided in this paper (Tables 1, 2; Appendix 1).

OVERVIEW

Phase 2 magmatism in the Macquarie Arc commenced in the Darriwilian Da2–Da3 interval of the Middle Ordovician, around 465–467 Ma, and involved mainly high-K calc-alkaline magmatism with both volcanic and intrusive expression. A tectono-magmatic event between 456 and 441 Ma, from the Eastonian to late Bolindian, terminated Phase 2 magmatism and is associated with widespread emplacement of Phase 3 relatively small-volume but distinctive medium-K dacites and granodiorites (the Copper Hill Suite), accompanied by regional uplift, erosion and limestone deposition. In the Junee–Narromine Volcanic Belt and western Molong Volcanic Belt, limestones separate Phase 2 magmatic products from the overlying Phase 4 volcanics. The latter magmatic episode post-dated *ca* 452 Ma and extended to the age of the youngest dated porphyries, which is 437 Ma (earliest Silurian) in the Junee–Narromine Volcanic Belt.

This paper is built around Figure 2, a lithostratigraphic column for the Macquarie Arc showing magmatic affinities of each key volcanic unit. Thorough descriptions of key lithostratigraphic units in these volcanic belts are given in Clarke (1990), Krynen *et al.* (1990), Miles and Brooker (1998), Pogson and Watkins (1998), Raymond *et al.* (1998), Meakin and Morgan (1999), Morgan *et al.* (1999), Lyons and Wallace (1999), Lyons *et al.* (2000), Percival (2000), Percival *et al.* (1999), Raymond and Sherwin (1999), Sherwin (1996), Simpson *et al.* (2005) and in accompanying papers in this thematic issue, and we do not repeat these here, except where our new mapping has delineated geological relationships that differ from, or significantly add to, published information. Our mapping and sampling concentrated on the best exposed, most informative sections of each volcanic belt, and are supplemented by drillhole information and sampling in areas of little or no outcrop. Here we report on the temporal variation of magmatic affinities of dominant units representing Phases 2, 3, and 4 magmatism in key areas of each of the three main volcanic belts of the Macquarie Arc.

Arc and arc-like magmatic suites are usually classified into low-K, medium-K calc-alkaline, high-K calc-alkaline, or shoshonitic affinities using a K_2O-SiO_2 plot. However, the mobility of K_2O in regional metamorphism and localised hydrothermal alteration is well known and introduces a significant complication into applying this system to ancient volcanic and shallow intrusive rocks such as those studied from the Macquarie Arc, even for carefully selected least altered rocks. A further complexity is that many lava suites for which we have comprehensive analytical data from modern southwest Pacific (e.g. Vanuatu) and Sunda (Indonesian) arc volcanoes tend to cross the conventional field boundaries defined on the K_2O-SiO_2 plot. For example, basalts from Tanna Island in the southern Vanuatu arc plot in the medium-K calc-alkaline field, comagmatic basaltic andesites and more mafic andesites plot in the high-K field, and the evolved andesites and dacites in the same volcano plot in the shoshonitic field (Figure 3a). Our available data suggest that arc magmatic suites tend to broadly parallel the field boundaries on the K_2O-SiO_2 plot for regions underlain by continental crust or thick arc crust, but suites erupted in thin oceanic arcs with ocean crust basement tend to plot across the field boundaries in the manner shown by the Tanna suite. Furthermore, many lava suites in post-collisional and arc–rift settings show rapid and repeated compositional shifts between high-K calc-alkaline and shoshonitic series lavas (e.g. Raki Raki volcano and adjacent cones, Fiji: A. J. Crawford & R. J. Squire unpubl. data).

To enable a valid assignment of magmatic affinities bearing relation to the K_2O-SiO_2 plot, and based on the accepted immobility of Al_2O_3, where appropriate we use a P_2O_5/Al_2O_3 *vs* K_2O/Al_2O_3 plot based on 11 volcanoes from the modern Vanuatu–Fiji region, and 10 volcanoes from the Sunda arc to define fields keyed to well-known fields on the K_2O-SiO_2 plot (Figure 3b). Samples of Macquarie Arc lavas that have undergone K_2O depletion will be shifted to the left of the polygon that accommodates >99% of our modern arc dataset. Of course, due to the slope of the field boundaries on this plot, some K_2O loss might shift (for example) a shoshonitic lava into the high-K field, but as shown by the Goonumbla and Wombin Volcanics in Figure 3a, b, this is unlikely to compromise interpretation of the entire suite. Thus, these ancient volcanic and shallow intrusive suites are defined on the basis of their dominant lava population.

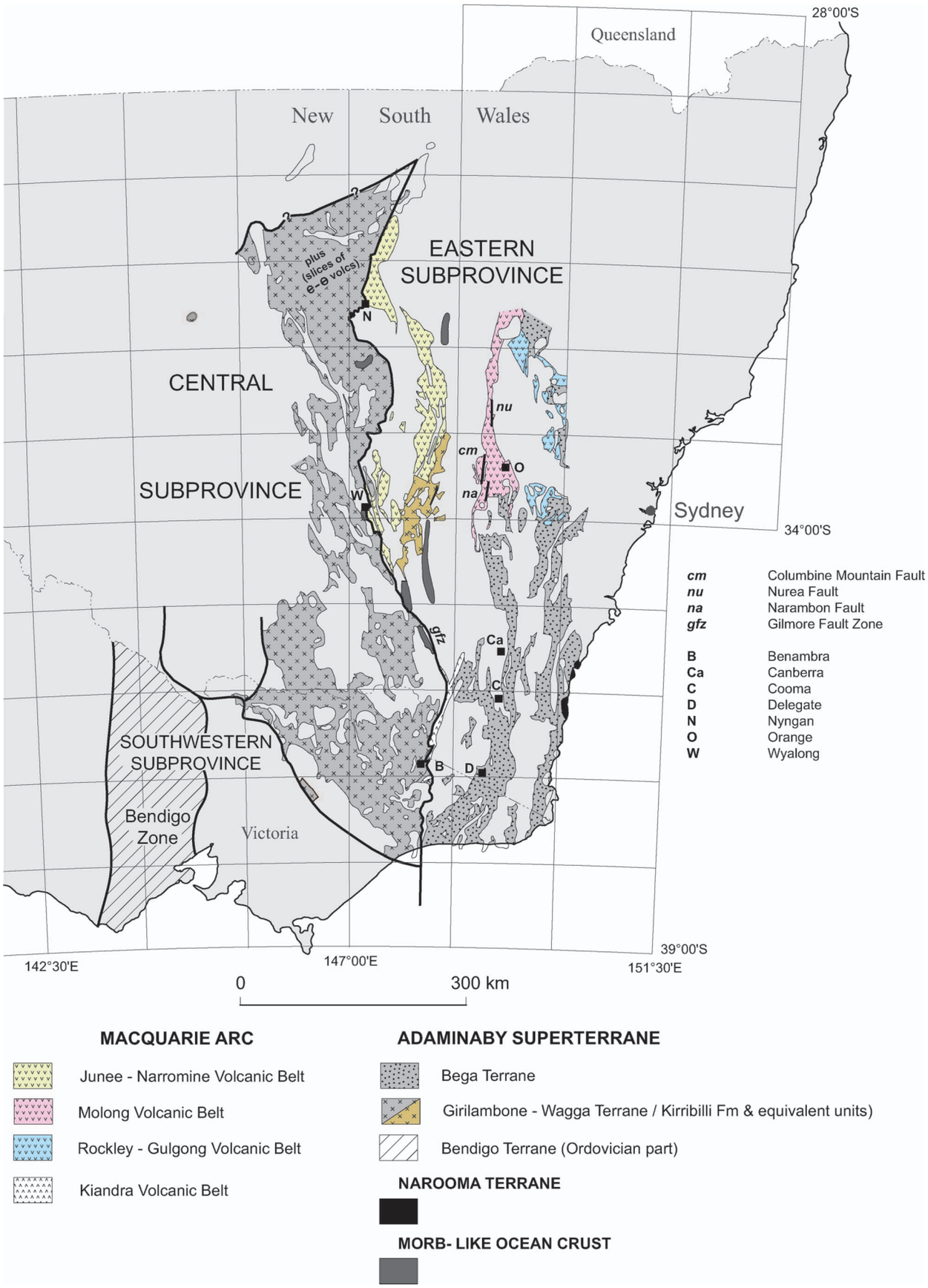

Figure 1 Elements of the now disrupted Ordovician to Early Silurian Macquarie Arc in the Central and Eastern Subprovinces of the Lachlan Orogen, showing the Junee–Narromine, Molong, Rockley–Gulgong and Kiandra Volcanic Belts.

Downloaded by [Auckland University of Technology] at 15:24 09 March 2015

Table 1 Representative whole-rock major- and trace-element analyses, recalculated loss-on-ignition (LOI)-free, for Middle and Late Ordovician igneous rocks from the Macquarie Arc (see Appendix 1 for location and rock type of samples).

	Goonumbla Volcanics							Wombin Volcanics			Post-Min E37 Zero trachyte
	Basal Mafic Unit										
Sample no.	CSG112	CSG23	CSG88	10-22-1	CSG100	CSG89	CSG141B	CSG12	CSG107	10-22-12	E37H3-245.2
SiO_2	51.81	54.75	56.87	55.33	59.92	53.00	56.02	53.77	57.26	61.76	66.68
TiO_2	0.53	0.66	0.62	0.68	0.49	0.76	0.81	0.76	0.56	0.41	0.29
Al_2O_3	14.59	16.90	15.82	18.96	17.99	18.53	18.00	19.57	19.14	18.64	16.66
Fe_2O_3	9.68	8.69	8.37	6.34	5.84	8.74	8.28	7.41	5.66	3.89	2.92
MnO	0.17	0.16	0.14	0.16	0.14	0.15	0.22	0.17	0.24	0.09	0.05
MgO	6.07	4.93	3.93	2.67	2.26	3.44	3.71	2.94	1.76	0.82	1.60
CaO	11.43	7.76	6.96	5.98	4.89	6.20	2.91	6.87	4.85	2.30	1.96
Na_2O	2.38	3.22	4.06	5.27	4.32	5.08	6.28	4.19	6.52	6.50	4.15
K_2O	2.87	2.51	2.76	3.24	3.81	2.22	0.74	3.66	3.62	5.28	5.51
P_2O_5	0.40	0.35	0.39	0.42	0.29	0.37	0.22	0.54	0.30	0.22	0.10
LOI	3.96	1.47	1.97	1.68	2.37	2.02	3.92	0.59	4.70	3.17	3.18
Ni	54	47	80	4	9	7	9	4	2	2	2
Cr	228	125	219	4	6	9	13	4	3	2	5
V	282	217	193	209	230	139	191	195	155	72	68
Sc	28	17	20	8	16	14	21	13	8	6	4
Zr	36	93	101	122	98	124	127	86	130	151	98
Nb	3.7	6.6	6.6	8.3	6.2	8.7	8.8	5.7	8.7	8.5	6.1
Y	12	17	17	21	17	21	23	21	21	22	12
Sr	949	1083	1093	1355	1408	1043	955	1587	648	526	171
Rb	37	21	36	53	58	36	8	60	42	77	83
Ba	611	549	653	865	931	883	150	971	818	832	988
Pb	5	5	7	6	11	4	2	9	6	12	2
Zn	79	86	75	90	61	100	86	77	62	81	48
Cu	157	172	156	181	34	152	149	101	102	14	8
Nb	*4.31*	*6.22*	*6.88*	*8.36*	*5.74*	*9.04*	*8.82*	*6.06*	*8.74*	*8.92*	*6.41*
Hf	*1.03*	*2.56*	*2.62*	*3.04*	*2.8*	*3.14*	*3.13*	*2.31*	*3.22*	*3.77*	*2.00*
Ta	*0.24*	*0.38*	*0.41*	*0.53*	*0.37*	*0.55*	*0.55*	*0.37*	*0.5*	*0.54*	*0.45*
Pb	*4.94*	*7.24*	*7.37*	*8.81*	*11.25*	*5.61*	*2.83*	*11.26*	*5.71*	*14.94*	*3.36*
Th	*1.66*	*2.41*	*2.65*	*3.73*	*3.27*	*2.64*	*2.08*	*3.02*	*3.39*	*4.84*	*3.27*
U	*0.73*	*1.16*	*1.07*	*1.84*	*1.78*	*1.26*	*1.21*	*1.51*	*0.97*	*1.73*	*1.01*
La	*11.19*	*14.8*	*15.83*	*17.2*	*17.9*	*15.56*	*14.8*	*18.92*	*17.42*	*20.94*	*13.14*
Ce	*19.26*	*28.56*	*29.12*	*32.73*	*33.25*	*30.11*	*30.3*	*36.07*	*31.2*	*38.52*	*20.47*
Pr	*2.33*	*3.54*	*3.70*	*4.12*	*4.08*	*3.9*	*4.03*	*4.46*	*3.81*	*4.7*	*2.27*
Nd	*9.99*	*15.97*	*16.12*	*17.28*	*16.42*	*17.13*	*18.17*	*20.17*	*16.07*	*18.64*	*8.78*
Sm	*2.35*	*3.71*	*3.59*	*3.91*	*3.63*	*4.01*	*4.29*	*4.56*	*3.57*	*4.10*	*1.70*
Eu	*0.78*	*1.09*	*1.04*	*1.25*	*1.14*	*1.26*	*1.24*	*1.46*	*1.17*	*1.15*	*0.54*
Gd	*2.31*	*3.41*	*3.32*	*4.13*	*3.79*	*3.86*	*4.09*	*4.36*	*3.47*	*3.72*	*1.63*
Tb	*0.36*	*0.54*	*0.51*	*0.59*	*0.51*	*0.63*	*0.67*	*0.66*	*0.58*	*0.62*	*0.24*
Dy	*2.17*	*3.19*	*2.97*	*3.47*	*2.97*	*3.84*	*4.15*	*3.91*	*3.55*	*3.59*	*1.49*
Ho	*0.47*	*0.65*	*0.65*	*0.74*	*0.63*	*0.83*	*0.90*	*0.82*	*0.79*	*0.77*	*0.35*
Er	*1.34*	*1.87*	*1.78*	*2.14*	*1.89*	*2.28*	*2.52*	*2.26*	*2.28*	*2.27*	*1.11*
Tm	*0.19*	*0.27*	*0.27*	*0.31*	*0.28*	*0.35*	*0.38*	*0.33*	*0.34*	*0.35*	*0.18*
Yb	*1.27*	*1.84*	*1.76*	*2.11*	*1.87*	*2.26*	*2.47*	*2.16*	*2.35*	*2.35*	*1.29*
Lu	*0.20*	*0.28*	*0.28*	*0.33*	*0.30*	*0.34*	*0.38*	*0.33*	*0.37*	*0.37*	*0.22*

Major- and trace-element analyses by XRF, except for italicized trace elements which are by IC-PMS. (*continued*)

Downloaded by [Auckland University of Technology] at 15:24 09 March 2015

For example, the Goonumbla and Wombin Volcanics of the Junee–Narromine Volcanic Belt are unambiguously shoshonitic, whereas the Walli Volcanics lavas of the southern Molong Volcanic Belt show both high-K and shoshonitic affinities.

In a similar fashion, we also use a P_2O_5 *vs* MgO plot (Figure 3c) based on the same modern arc lava suites to discriminate magmatic affinities keyed to K_2O-SiO_2 relationships: note that this diagram cannot be used for suites where apatite is a fractionating phase (usually for lavas with $<3\%$ MgO), and that it cannot effectively and consistently separate high-K calc-alkaline suites from shoshonitic suites.

MIDDLE ORDOVICIAN GEOLOGY AND LITHOSTRATIGRAPHY

Junee–Narromine Volcanic Belt

The Junee–Narromine Volcanic Belt has been interpreted to be the core of the Macquarie Arc, being

Table 1 (*Continued*).

	Parkes Volcanics				Bushman Volcanics				Nash Hill Volcanics			
Sample no.	BV5	BV7	BV8	BV6	W1288A	10-18-1	BV1	BV3	NH19	NH15	NH18	NH21
SiO_2	54.08	53.21	58.00	69.20	59.65	53.53	54.48	63.31	51.06	63.76	53.41	51.75
TiO_2	0.95	1.02	0.85	0.22	0.44	0.50	0.48	0.36	0.86	0.60	0.78	0.87
Al_2O_3	18.10	19.38	17.05	17.90	15.08	17.23	18.52	15.13	11.75	14.37	18.69	17.71
Fe_2O_3	11.39	12.73	8.71	1.90	6.21	10.23	8.29	6.31	11.58	6.63	8.21	9.91
MnO	0.13	0.16	0.11	0.01	0.14	0.18	0.17	0.12	0.19	0.09	0.13	0.14
MgO	4.73	5.56	3.49	0.86	3.42	5.24	3.67	1.99	8.59	2.38	3.33	4.17
CaO	4.22	1.01	4.54	0.47	14.72	9.70	5.63	8.18	11.92	7.91	8.53	7.90
Na_2O	5.80	6.38	6.68	8.59	0.13	2.15	4.27	4.10	1.94	3.55	4.73	1.99
K_2O	0.15	0.08	0.19	0.77	0.04	1.01	3.81	0.12	1.62	0.37	1.77	4.74
P_2O_5	0.42	0.46	0.40	0.09	0.14	0.17	0.50	0.37	0.31	0.22	0.34	0.47
LOI	6.81	1.03	4.92	1.39	4.28	4.57	2.08	2.85	2.25	2.91	2.70	1.23
Ni	25	27	29	10	20	9	7	3	50	8	5	15
Cr	57	62	79	10	151	26	17	12	334	13	5	22
V	302	210	268	44	190	368	301	218	330	253	266	366
Sc	27	32	25	4	29	40	33	25	42	32	29	31
Zr	154	164	143	141	55	45	118	116	71	52	105	116
Nb	5	5.1	4.8	24.2	5.3	2.5	9.2	8.1	9.3	5.3	13.7	19.5
Y	23	23	21	11	12	11	18	23	17	17	19	19
Sr	502	349	483	604	117	677	1478	1687	343	435	675	1313
Rb	2		2	8	2	26	57	8	21	7	46	75
Ba	54	207	145	207	190	658	1808	64	1791	1409	548	3581
Pb	6	4	5		19	9	5	2	16	21	9	7
Zn	116	127	78	19	51	87	100	86	92	48	74	89
Cu	131	111	105	49	41	104	78	149	136	93	112	137
Nb	*4.41*		*4.21*	–	–	–	*9.20*	*8.13*	*10.64*	*6.37*	*15.17*	*21.87*
Hf	*4.21*		*4.09*	–	–	–	*3.22*	*2.79*	*1.86*	*1.45*	*2.52*	*2.81*
Ta	*0.20*		*0.18*	–	–	–	*0.40*	*0.23*	*0.45*	*0.34*	*0.77*	*1.05*
Pb	*6.20*		*5.20*	–	–	–	*4.90*	*12.60*	*19.34*	*27.85*	*15.01*	*18.33*
Th	*1.91*		*1.75*	–	–	–	*12.89*	*12.51*	*7.76*	*10.59*	*14.1*	*24.72*
U	*1.22*		*1.02*	–	–	–	*2.74*	*4.48*	*2.21*	*2.63*	*3.78*	*4.80*
La	*16.93*		*16.12*	–	–	–	*46.15*	*54.28*	*34.98*	*37.39*	*50.94*	*58.66*
Ce	*41.43*		*40.78*	–	–	–	*96.06*	*98.77*	*63.43*	*58.30*	*85.59*	*102.02*
Pr	*5.15*		*4.83*	–	–	–	*9.80*	*9.57*	*7.80*	*6.29*	*9.77*	*11.51*
Nd	*25.86*		*23.78*	–	–	–	*41.91*	*39.61*	*30.78*	*23.57*	*36.74*	*42.03*
Sm	*5.47*		*4.99*	–	–	–	*7.08*	*6.33*	*6.04*	*4.09*	*6.47*	*7.00*
Eu	*1.50*		*1.37*	–	–	–	*1.88*	*1.71*	*1.77*	*1.12*	*1.75*	*1.88*
Gd	*4.48*		*4.10*	–	–	–	*5.06*	*4.35*	*5.95*	*4.21*	*4.99*	*6.89*
Tb	*0.61*		*0.58*	–	–	–	*0.63*	*0.55*	*0.65*	*0.44*	*0.63*	*0.68*
Dy	*3.37*		*3.18*	–	–	–	*3.19*	*2.84*	*3.42*	*2.49*	*3.47*	*3.6*
Ho	*0.65*		*0.61*	–	–	–	*0.55*	*0.50*	*0.67*	*0.53*	*0.70*	*0.74*
Er	*1.81*		*1.70*	–	–	–	*1.43*	*1.39*	*1.82*	*1.50*	*2.10*	*2.05*
Tm	*0.26*		*0.24*	–	–	–	*0.19*	*0.19*	*0.25*	*0.21*	*0.28*	*0.28*
Yb	*1.74*		*1.64*	–	–	–	*1.27*	*1.42*	*1.55*	*1.39*	*1.86*	*1.87*
Lu	*0.27*		*0.25*	–	–	–	*0.19*	*0.23*	*0.23*	*0.22*	*0.29*	*0.28*

(*continued*)

composed of large volumes of volcanic rocks interpreted as an imbricate stack of thrust sheets (Glen *et al.* 1998, 2007b; Direen *et al.* 2001). We focus on the section between Forbes and just north of Peak Hill in the central section of the belt, where it has a strong magnetic expression that extends at least to just north of Nyngan, and semicontinuous, albeit generally fairly poor, exposures of Ordovician volcanics rocks. Large blocks of similar aged rocks occur under cover at the northern (Narromine Igneous Complex) and southern (Cowal and Fairholme Igneous Complexes) ends of this belt, and are only known from limited, shallow RAB drilling and more informative diamond drillcores from around the Cowal deposit and exploration in the Narromine Igneous Complex (Crawford *et al.* 2007).

PARKES–FORBES AREA, WEST OF THE PARKES THRUST

Phase 1 Lower Ordovician Nelungaloo Volcanics and the overlying Bendigonian Yarrimbah Formation constitute an upward-fining sequence that is interpreted to end with either cessation of, or a major hiatus in, arc magmatism (Glen *et al.* 2007a; Simpson *et al.* 2005). The poorly exposed base of the Middle Ordovician Phase 2 rocks is marked by volcaniclastic sandstones and siltstones that pass up into the Billabong Creek Limestone with rare interbedded basaltic andesite lavas and volcaniclastic sediments (Figure 2).

The volcanic–volcaniclastic succession stratigraphically above and interfingering with the Billabong Creek Limestone has been assigned to the Goonumbla Volca-

Downloaded by [Auckland University of Technology] at 15:24 09 March 2015

Table 1 (*Continued*).

	Northparkes Igneous Complex											
	Intrusions (Regional)				Lower Blayney Volcanics					Upper Blayney Volcanics		
Sample no.	CGS11	CSG59B	CSG189	E28H13-53.8	MB98	PBD3	PBD52	PBD15\	MB3	RSMB5	MB12	MB80
SiO_2	52.40	52.34	59.76	62.36	51.01	55.36	51.41	53.21	51.73	50.62	50.06	51.23
TiO_2	0.82	0.80	0.47	0.47	0.49	0.68	0.57	0.43	0.45	0.52	0.42	0.46
Al_2O_3	19.66	17.57	18.17	18.71	13.63	14.99	11.61	12.86	10.68	10.90	11.15	10.27
Fe_2O_3	8.13	9.29	5.51	5.60	9.84	8.65	10.40	8.72	11.60	12.42	11.75	12.09
MnO	0.21	0.19	0.17	0.11	0.16	0.13	0.21	0.17	0.18	0.20	0.30	0.16
MgO	3.36	4.32	2.05	2.36	10.66	6.82	11.15	9.00	9.33	10.99	10.51	10.15
CaO	7.27	7.60	4.77	1.01	11.58	6.96	10.67	10.76	8.95	9.10	12.05	10.19
Na_2O	4.26	3.33	4.68	4.86	1.71	5.62	2.30	2.81	0.81	3.08	1.24	3.12
K_2O	3.19	4.04	4.04	3.79	0.70	0.53	1.45	1.83	5.84	1.79	2.12	1.92
P_2O_5	0.57	0.42	0.29	0.31	0.20	0.26	0.24	0.21	0.43	0.38	0.42	0.42
LOI	2.64	1.88	0.81	2.49	1.90	1.73	2.75	2.17	1.72	2.25	2.02	1.55
Ni	5	13	6	4	213	83	207	92	103	125	106	99
Cr	6	21	9	3	877	307	755	505	443	527	564	480
V	221	271	128	161	238	248	268	211	288	250	268	261
Sc	14	20	10	10	36	32	35	39	37	34	38	39
Zr	67	85	112	119	43	64	47	37	25	36	23	21
Nb	4.5	5	6.1	6.5	3.9	5.4	3.4	3.0	1.9	2.5	1.7	1.7
Y	20	20	18	16	12.0	18.0	15.0	11.0	13.0	13.0	10.1	11.0
Sr	1731	1538	1016	880	405	251	339	323	820	289	491	539
Rb	53	54	58	70	13.0	8.5	21.4	30.2	81.0	24.2	28.5	29.0
Ba	1124	949	842	1165	409	369	726	1011	1426	249	957	363
Pb	4	4	9	8	–	1.8	1.9	1.9	–	5.0	2.3	–
Zn	86	95	92	142	–	74	80	73	–	99	102	–
Cu	104	190	62	1078	–	121	107	110	–	53	84	–
Nb	*4.66*	*5.19*	*5.51*	–	–	*4.47*	*3.57*	*3.02*	–	–	–	*1.09*
Hf	*2.01*	*2.45*	*3.24*	–	–	*1.61*	*1.22*	*0.97*	–	–	–	*0.67*
Ta	*0.39*	*0.44*	*0.53*	–	–	–	–	–	–	–	–	*0.06*
Pb	*6.30*	*7.01*	*9.83*	–	–	*1.64*	*3.28*	*2.86*	–	–	–	*3.70*
Th	*2.1*	*2.54*	*3.54*	–	–	*1.46*	*1.10*	*0.98*	–	–	–	*0.57*
U	*1.02*	*1.29*	*2.07*	–	–	*0.69*	*0.52*	*0.45*	–	–	–	*0.27*
La	*18.2*	*15.74*	*18.41*	–	–	*10.00*	*7.34*	*6.19*	–	–	–	*4.79*
Ce	*34.70*	*30.10*	*33.82*	–	–	*20.20*	*14.70*	*12.30*	–	–	–	*9.60*
Pr	*4.70*	*4.06*	*4.32*	–	–	*2.59*	*1.94*	*1.59*	–	–		*1.33*
Nd	*20.50*	*17.53*	*17.70*	–	–	*11.10*	*8.47*	*6.82*	–	–	–	*6.20*
Sm	*4.74*	*4.15*	*3.77*	–	–	*2.77*	*2.17*	*1.76*	–	–	–	*1.81*
Eu	*1.50*	*1.23*	*1.14*	–	–	*0.71*	*0.66*	*0.55*	–	–	–	*0.64*
Gd	*4.53*	*4.09*	*3.5*	–	–	*2.98*	*2.40*	*1.94*	–	–	–	*2.07*
Tb	*0.70*	*0.67*	*0.55*	–	–	*0.50*	*0.41*	*0.33*	–	–	–	*0.33*
Dy	*3.80*	*3.73*	*3.14*	–	–	*3.10*	*2.49*	*2.00*	–	–	–	*1.92*
Ho	*0.75*	*0.75*	*0.64*	–	–	*0.67*	*0.55*	*0.44*	–	–	–	*0.40*
Er	*2.21*	*2.27*	*2.04*	–	–	*1.97*	*1.60*	*1.27*	–	–	–	*1.10*
Tm	–	–	–	–	–	–	–	–	–	–	–	–
Yb	*1.97*	*2.13*	*2.08*	–	–	*1.85*	*1.56*	*1.22*	–	–	–	*1.05*
Lu	*0.31*	*0.34*	*0.34*	–	–	*0.29*	*0.24*	*0.19*	–	–	–	*0.16*

(*continued*)

nics, the lower section of the Northparkes Group (Percival & Glen 2007). The earliest Goonumbla Volcanics are basaltic andesite lavas occurring just below Da3/4 boundary limestones in the upper Billabong Creek Limestone (Percival & Glen 2007), indicating an eruption age of *ca* 463 Ma (Figure 2).

Goonumbla Volcanics

Volcaniclastic-dominated sequences stratigraphically above the Phase 1 Nelungaloo Volcanics have previously been assigned to the Goonumbla Volcanics and overlying Wombin Volcanics. These units, together with mainly comagmatic small stocks and finger-like intrusions, form the Northparkes Group (Percival & Glen 2007) and have been described in detail by Krynen *et al.* (1990) and Simpson *et al.* (2005). The latter authors suggested that the entire complex probably represents a single volcanic edifice. The Wombin Volcanics, as originally defined, extend well west of the Goonumbla Volcanics and were differentiated from the latter on the rather tenuous basis that they are generally brick red, and more latitic than the trachyandesitic Goonumbla Volcanics. However, Simpson *et al.* (2005) and our own

Downloaded by [Auckland University of Technology] at 15:24 09 March 2015

Table 1 (*Continued*).

	Millthorpe Volcanics			
Sample no.	PBD21	PBD39	PBD42	PBD56
SiO_2	55.28	60.66	51.36	53.64
TiO_2	0.53	0.42	0.73	0.75
Al_2O_3	15.91	13.13	16.99	15.9
Fe_2O_3	8.78	7.87	10.86	9.57
MnO	0.13	0.14	0.18	0.13
MgO	3.98	2.67	4.54	5.17
CaO	7.1	8.48	7.98	6.93
Na_2O	4.88	3.65	2.76	4.35
K_2O	2.98	2.55	4.08	3.22
P_2O_5	0.43	0.42	0.52	0.32
LOI	1.93	2.08	2.75	2.16
Ni	19	14	14	23
Cr	60	57	18	54
V	275	225	311	266
Sc	28	26	28	29
Zr	50	30	59	60
Nb	4	3	6	7
Y	13	11	18	15
Sr	697	528	1195	620
Rb	38	35	66	47
Ba	1042	752	1302	789
Pb	5	4	4	2
Zn	74	48	49	70
Cu	86	89	65	71
Nb	*4.48*	*3.11*	*5.74*	*7.02*
Hf	*1.37*	*0.87*	*1.58*	*1.48*
Ta	–	–	–	–
Pb	*5.29*	*4.31*	*4.82*	*4.51*
Th	*1.85*	*1.13*	*1.51*	*1.95*
U	*0.79*	*0.55*	*0.50*	*0.62*
La	*12.00*	*9.23*	*12.10*	*9.97*
Ce	*22.00*	*16.60*	*22.50*	*19.50*
Pr	*2.68*	*2.03*	*2.78*	*2.48*
Nd	*11.10*	*8.24*	*11.75*	*10.70*
Sm	*2.48*	*1.98*	*2.86*	*2.67*
Eu	*0.79*	*0.63*	*0.90*	*0.85*
Gd	*2.61*	*2.10*	*3.13*	*2.88*
Tb	*0.41*	*0.33*	*0.51*	*0.46*
Dy	*2.53*	*1.98*	*3.17*	*2.79*
Ho	*0.54*	*0.44*	*0.69*	*0.59*
Er	*1.56*	*1.25*	*2.03*	*1.68*
Tm	–	–	–	–
Yb	*1.52*	*1.23*	*1.97*	*1.58*
Lu	*0.23*	*0.19*	*0.31*	*0.24*

(*continued*)

data and observations indicate that many of the thick grey trachyandesites mapped as a key component of the Goonumbla Volcanics are probably subvolcanic sills erupted late in the magmatic episode (our Phase 4), and that the Goonumbla trachyandesites and Wombin Volcanics trachyandesites and trachytes are essentially comagmatic.

With these intrusive units removed from the stratigraphic section, Phase 2 magmatism in the Goonumbla Volcanics is represented by a succession of thin basaltic andesite flows informally referred to as the basal mafic unit, with some volcanic conglomerate and minor finer grained volcaniclastics. The basal mafic unit lavas in the Goonumbla Volcanics differ from the more evolved (trachyandesitic and trachytic) Wombin Volcanics lavas and sills higher in the sequence in lacking apatite phenocrysts and containing uncommon altered olivine phenocrysts. Small monzodiorite intrusions in the Nelungaloo, Goonumbla and Wombin Volcanics are mainly related to post-445 Ma Phase 4 magmatism, but we note that Butera *et al.* (2001) also recorded a SHRIMP zircon U–Pb age of 450.8 ± 4.2 Ma for one monzodiorite intrusion from the Northparkes area.

The Goonumbla Volcanics basal mafic unit lavas (Table 1) plot in the high-K calc-alkaline and shoshonitic fields (Figure 3a–c). The rare-earth elements (REE) are considered to be immobile at the low grade of alteration shown by the rocks analysed for this study. In terms of REE patterns (Figure 3d), the basal mafic unit basaltic andesites show patterns very close to, but with slightly stronger LREE enrichment than, the average Fijian Late Miocene shoshonite at MgO 6% (Rogers & Setterfield 1994; Verbeeten 1996). Age-corrected initial ε_{Nd} values for the Nelungaloo Volcanics are +7.3 to +7.5 (Glen *et al.* 2007a), whereas the one analysed Goonumbla Volcanics basic mafic unit lava has a value of +6.0 (Table 2).

Phase 4 trachyandesite sills in the upper part of the Goonumbla Volcanics, and the overlying Wombin Volcanics are remarkably homogeneous, moderately porphyritic trachyandesites and trachytes that show plagioclase + augite + FeTiOx-phyric phenocryst assemblages, with ubiquitous stout apatite microphenocrysts that persist across the compositional spectrum from trachyandesite to trachyte. Fresh or altered biotite phenocrysts are common in many of the more evolved lavas, and several better preserved trachytes have sanidine phenocrysts, although these are subordinate to plagioclase. Hornblende phenocrysts are rare. Groundmasses are almost always crystalline. The uppermost lavas include rare subaerial trachytic ignimbrites. Formerly glassy groundmasses are common in more evolved, banded, trachytic lavas in which spherulitic textures are commonly well preserved. The deep-red colour of many Wombin Volcanics is due to pervasive microcrystalline hematite dust in both phenocrystal and groundmass feldspars. Late intrusive monzonites in the Wombin Volcanics show similar red coloration (Lickfold *et al.* 2007).

The following key points are noted with respect to the upper Goonumbla (trachyandesitic sills) and Wombin Volcanics (Table 1).

(1) The Goonumbla Volcanics trachyandesite sills and Wombin Volcanics are broadly a comagmatic package for which K_2O–SiO_2 relationships, Al_2O_3-normalised P_2O_5 contents and P_2O_5–MgO relationships define a pronounced shoshonitic affinity (Figure 3a–c). Many of the brick-red, formerly glassy trachytes (and late intrusive monzonites) have K_2O up to 7%, and have clearly undergone post-magmatic K_2O-enrichment (Figure 3b). The Goonumbla and Wombin Volcanics trachyandesite REE patterns (Figure 3d) show similar strongly LREE-enriched patterns to the basal mafic unit, and are generally slightly more LREE-enriched than patterns for Fijian shoshonites with 3–6% MgO. A shoshonitic affinity for the bulk of the Goonumbla and Wombin Volcanics is beyond doubt, and is supported by the work of Blevin (2002), Müller and Groves (2000), and

Downloaded by [Auckland University of Technology] at 15:24 09 March 2015

Table 1 (*Continued*).

	Byng Volcanics							Coombing Formation dykes	
Sample no.	RDW170	RDW193	RDW80	RDW142	RDW119	RDW178	RDW140	BLRS0139	BLRS0189
SiO_2	55.38	54.49	48.62	49.06	47.82	44.55	45.58	50.98	51.75
TiO_2	0.55	0.42	0.43	0.37	0.23	0.16	0.07	0.42	0.40
Al_2O_3	14.97	11.43	9.80	7.74	5.89	2.50	0.52	12.25	10.56
Fe_2O_3	8.89	10.96	12.17	12.77	12.48	16.36	14.71	10.40	10.59
MnO	0.14	0.14	0.20	0.18	0.17	0.21	0.20	0.19	0.19
MgO	3.68	7.54	14.92	18.68	24.24	28.95	34.54	10.36	9.23
CaO	7.51	9.57	8.75	8.80	8.66	7.08	4.27	11.20	13.67
Na_2O	2.76	4.24	1.66	0.84	0.22	0.14	0.11	1.56	2.36
K_2O	5.53	0.76	3.08	1.20	0.02	0.02	0.00	2.28	0.82
P_2O_5	0.60	0.44	0.37	0.36	0.25	0.02	0.01	0.41	0.45
LOI	0.94	1.18	2.12	5.68	5.73	8.55	8.78	1.76	0.91
Ni	30	67	275	388	1183	655	850	91	97
Cr	52	268	995	1457	2216	2131	2782	484	515
V	293	209	226	194	162	146	32	262	288
Sc	21	33	34	37	25	39	25	38	44
Zr	42	24	25	18	10	3	<1	23	19
Nb	1.9	1.6	1.5	1.3	<1	<1	<1	2.6	1.9
Y	13.0	9.0	10.0	8.0	6.0	5.0	–	10.8	10.5
Sr	1062	630	477	360	119	54	8	666	708
Rb	68.0	7.0	54.0	51.0	<1	2.0	<1	31.8	10.9
Ba	631	2756	551	144	36	481	28	808	539
Pb	20.0	7.0	2.0	2.0	5.0	<1.5	<1.5	3.8	4.1
Zn	68	44	95	75	55	–	–	85	72
Cu	50	134	13	8	60	26	12	115	124
Nb	*2.04*	*1.06*	*1.01*	*0.76*	*0.55*	*0.09*	*0.01*	*2.78*	–
Hf	*1.02*	*0.65*	*0.67*		*0.30*	*0.13*	*0.02*	*0.62*	–
Ta	–	–	–	*2.02*	–	–	–	*0.16*	–
Pb	*21.42*	*8.54*	*2.53*	*0.58*	*3.29*	*0.36*	*0.52*	*4.05*	–
Th	*1.53*	*0.72*	*0.69*	*0.20*	*0.30*	*0.01*	*0.00*	*2.09*	–
U	*0.53*	*0.34*	*0.30*	–	*0.22*	*0.02*	*0.00*	–	–
La	*10.14*	*4.72*	*6.06*	*3.78*	*2.48*	*0.79*	*0.14*	*9.33*	–
Ce	*19.30*	*9.16*	*11.40*	*7.29*	*4.94*	*1.70*	*0.32*	*15.84*	–
Pr	*2.42*	*1.24*	*1.59*	*1.01*	*0.73*	*0.31*	*0.05*	*1.82*	–
Nd	*10.32*	*5.79*	*7.11*	*4.53*	*3.29*	*1.76*	*0.36*	*7.30*	–
Sm	*2.74*	*1.76*	*2.00*	*1.30*	*0.88*	*0.64*	*0.13*	*1.71*	–
Eu	*0.82*	*0.62*	*0.70*	*0.40*	*0.30*	*0.27*	*0.06*	*0.55*	–
Gd	*2.75*	*2.03*	*2.36*	*1.49*	*1.03*	*0.89*	*0.19*	*1.86*	–
Tb	*0.43*	*0.31*	*0.38*	*0.24*	*0.17*	*0.14*	*0.03*	*0.31*	–
Dy	*2.47*	*1.79*	*2.25*	*1.42*	*1.00*	*0.79*	*0.19*	*1.87*	–
Ho	*0.51*	*0.38*	*0.48*	*0.29*	*0.21*	*0.18*	*0.04*	*0.39*	–
Er	*1.43*	*1.05*	*1.34*	*0.85*	*0.59*	*0.47*	*0.09*	*1.17*	–
Tm	–	–	–	–	–	–	–	–	–
Yb	*1.38*	*1.03*	*1.26*	*0.79*	*0.53*	*0.42*	*0.09*	*1.11*	–
Lu	*0.21*	*0.15*	*0.19*	*0.11*	*0.08*	*0.07*	*0.01*	*0.17*	–

(*continued*)

Müller *et al.* (1994). The latter authors argued that the Goonumbla Volcanics best matched modern shoshonites formed in 'late oceanic arc' settings.

(2) Two lavas from the Goonumbla and Wombin Volcanics have age-corrected initial ε_{Nd} values (Table 2) of +5.8 and +6.0. A trachyte dyke, one of the zero porphyries (Lickfold *et al.* 2003, 2007) that cuts mineralisation at Northparkes in E37 and has a SHRIMP U–Pb zircon age of 437 ± 3.5 Ma (and is thus the youngest of the Wombin Volcanics), has an ε_{Nd} value of +5.0.

Numerous small plutons, plugs and dykes of monzodioritic to monzonitic rocks intruded the Goonumbla and Wombin Volcanics in the Late Ordovician to earliest Silurian. These rocks and their porphyry-style mineralisation (Lickfold *et al.* 2007; Cooke *et al.* 2007) have been dated mainly around 440 Ma, although at least one body has yielded an earlier U–Pb SHRIMP date of 450.8 ± 4.2 Ma (Butera *et al.* 2001). Most small plutons are composed of mainly plagioclase + augite-phyric rocks with subordinate K-feldspar (often rimming plagioclase), and commonly contain interstitial biotite, apatite, K-feldspar and FeTi oxides. Hornblende is distinctly less abundant than in similar intrusive rocks from the Narromine and Cowal Igneous Complexes. Quartz is locally present but is notably less abundant than in intrusive rocks from the Cowal Complex intrusives. Lickfold *et al.* (2003, 2007), and our

Downloaded by [Auckland University of Technology] at 15:24 09 March 2015

Table 1 (*Continued*).

	Cheesemans Creek Formation				Angullong Formation		Fairbridge Volcanics (Units 1–3 southern section)			
Sample no.	KA80	OR8	KA33	KA78	WA27	WA15	KA38a	OR12	OR61	OR95
SiO_2	54.81	55.18	55.17	55.57	51.71	58.55	49.22	48.64	52.11	52.88
TiO_2	0.67	0.62	0.59	0.61	0.91	0.64	0.60	0.61	0.69	0.67
Al_2O_3	17.26	17.01	19.52	18.54	17.41	17.76	13.60	12.86	14.14	13.87
Fe_2O_3	9.56	6.45	8.10	7.98	10.94	6.23	11.68	11.53	10.31	8.97
MnO	0.09	0.11	0.12	0.10	0.20	0.08	0.20	0.18	0.18	0.15
MgO	5.12	2.97	2.82	3.54	5.15	2.26	8.94	9.56	6.39	7.44
CaO	6.91	9.37	5.86	2.98	6.65	4.23	11.29	12.42	10.93	11.73
Na_2O	2.86	4.21	4.02	4.43	3.94	6.17	3.75	3.02	4.51	3.45
K_2O	2.38	3.75	3.26	5.66	2.77	3.83	0.52	0.91	0.49	0.56
P_2O_5	0.34	0.33	0.55	0.60	0.33	0.26	0.19	0.27	0.24	0.28
LOI	6.85	8.86	3.06	4.18	3.25	2.26	5.46	3.30	1.44	4.87
Ni	77	54	5	4	18	10	118	224	48	80
Cr	360	415	7	4	30	15	414	789	250	456
V	333	305	180	168	280	163	317	273	333	244
Sc	42	36	14	13	29	16	39	47	48	45
Zr	72	70	79	84	90	99	51	58	60	76
Nb	4.2	4.1	7.9	8.1	8.2	7.5	1.8	2.2	3.6	3.7
Y	14.9	14.7	18.4	19.6	21.8	16.6	14.2	13.7	17.4	19.2
Sr	752	872	1502	838	903	615	600	581	768	445
Rb	19.4	37.3	56.8	67.2	39.5	45.3	6.4	14.9	8.1	5.6
Ba	1579	1785	646	777	1072	1766	194	490	83	496
Pb	4.2	5.9	25.0	7.7	–	2.1	<1	7.8	3.4	4.7
Zn	96	83	91	99	99	66	90	109	95	76
Cu	125	119	156	162	96	34	118	300	29	101
Nb	–	–	*6.44*	–	*7.48*	–	–	–	–	–
Hf	–	–	*1.90*	–	*2.09*	–	–	–	–	–
Ta	–	–	*0.36*	–	*0.53*	–	–	–	–	–
Pb	–	–	*24.38*	–	*3.76*	–	–	–	–	–
Th	–	–	*4.99*	–	*1.82*	–	–	–	–	–
U	–	–	*1.83*	–	*0.60*	–	–	–	–	–
La	–	–	*22.90*	–	*13.20*	–	–	–	–	–
Ce	–	–	*41.10*	–	*24.50*	–	–	–	–	–
Pr	–	–	*4.96*	–	*3.05*	–	–	–	–	–
Nd	–	–	*19.90*	–	*12.90*	–	–	–	–	–
Sm	–	–	*3.85*	–	*3.09*	–	–	–	–	–
Eu	–	–	*1.24*	–	*1.08*	–	–	–	–	–
Gd	–	–	*3.69*	–	*3.72*	–	–	–	–	–
Tb	–	–	*0.55*	–	*0.64*	–	–	–	–	–
Dy	–	–	*3.07*	–	*3.87*	–	–	–	–	–
Ho	–	–	*0.65*	–	*0.83*	–	–	–	–	–
Er	–	–	*1.74*	–	*2.43*	–	–	–	–	–
Tm	–	–	–	–	–	–	–	–	–	–
Yb	–	–	*1.73*	–	*2.31*	–	–	–	–	–
Lu	–	–	*0.27*	–	*0.35*	–	–	–	–	–

(*continued*)

own data, show that intrusives into the Northparkes Group are a shoshonitic monzodiorite–monzonite suite comagmatic with the Goonumbla Volcanics trachyandesites and Wombin Volcanics (Figure 3a–c).

In summary, volcanic and high-level intrusive rocks in the central section of the Junee–Narromine Volcanic Belt include the late Darriwilian shoshonitic and high-K calc-alkaline basal mafic unit of the Goonumbla Volcanics representing Phase 2 magmatism, and an overlying sequence of volcaniclastic rocks. The latter are overlain and intruded by Phase 4 shoshonitic sills and lavas of the upper Goonumbla Volcanics–Wombin Volcanics and their comagmatic intrusive counterparts. These Phase 4 magmas are a Late Ordovician to Early Silurian (*ca* 445–437 Ma: Figure 2) shoshonitic suite in which the trachyandesites rarely have MgO >3%. Phase 3 medium-K high-level intrusive rocks are not known from this central section of the Junee–Narromine Volcanic Belt.

Mingelo Volcanics

The poorly known Mingelo Volcanics extend as a sparsely outcropping unit from Tomingley, north of Peak Hill, to the latitude of Parkes (Krynen *et al.* 1990; Glen *et al.* 2007c). Five analyses of lavas referred to as

Downloaded by [Auckland University of Technology] at 15:24 09 March 2015

Table 1 (*Continued*).

	Fairbridge Volcanics (Units 4–6 southern section)				Fairbridge Volcanics (Units 1–3 northern section)				Transitional alkaline dykes		
Sample no.	OR99	KA60	OR98	OR109	MB403	KA31	KA24	KA49	RS8–9	OR46	MB364
SiO_2	57.33	53.07	55.23	60.49	52.50	48.29	49.55	52.73	47.31	49.56	49.80
TiO_2	0.70	0.82	0.75	0.72	0.75	0.43	0.70	0.75	2.19	2.17	2.19
Al_2O_3	17.72	19.05	18.91	18.21	17.95	8.84	15.11	16.95	16.90	18.03	16.13
Fe_2O_3	8.66	8.87	7.79	6.17	10.01	10.96	11.20	9.35	12.41	7.95	10.25
MnO	0.14	0.14	0.16	0.07	0.16	0.17	0.19	0.19	0.22	0.16	0.17
MgO	3.79	3.85	3.01	2.12	6.73	17.10	6.43	5.83	6.99	4.49	7.50
CaO	7.20	6.14	8.77	3.18	5.40	13.57	12.42	9.09	10.37	11.71	7.81
Na_2O	3.61	4.17	4.39	7.36	5.86	0.43	2.96	3.09	2.76	4.31	4.82
K_2O	0.60	3.55	0.71	1.44	0.37	0.06	1.20	1.73	0.49	1.10	0.91
P_2O_5	0.24	0.34	0.27	0.22	0.27	0.15	0.24	0.31	0.35	0.51	0.42
LOI	5.52	3.32	5.78	3.36	5.65	15.83	3.14	2.44	2.72	4.87	5.57
Ni	10	16	11	10	30	368	66	44	85	56	111
Cr	16	33	17	11	173	1361	200	153	188	141	229
V	231	242	234	155	240	223	345	293	285	236	218
Sc	25	24	28	22	31	49	39	37	34	29	25
Zr	121	138	124	140	117	38	56	85	165	263	232
Nb	8.7	10.4	8.3	11.0	3.2	1.2	2.3	4.2	8.6	28.7	14.0
Y	19.5	20.8	19.9	16.2	20.2	9.5	15.9	19.3	29.9	29.3	27.7
Sr	702	804	872	664	286	230	753	642	345	505	463
Rb	7.0	51.3	8.3	20.2	2.4	<1	12.7	19.1	5.7	8.6	7.0
Ba	265	857	347	402	147	135	476	901	199	246	144
Pb	6.2	3.0	5.5	3.0	2.1	3.4	4.7	3.0	3.3	2.3	–
Zn	84	75	87	62	100	79	132	85	84	73	90
Cu	53	165	188	40	16	76	151	134	68	47	30
Nb	–	–	*7.53*	–	–	*1.01*	*1.90*	–	*8.64*	–	–
Hf	–	–	*2.82*	–	–	*0.86*	*1.41*	–	*3.72*	–	–
Ta	–	–	*0.51*	–	–	*0.06*	*0.11*	–	*0.59*	–	–
Pb	–	–	*4.95*	–	–	*2.72*	*3.36*	–	*2.01*	–	–
Th	–	–	*2.96*	–	–	*0.80*	*1.40*	–	*0.89*	–	–
U	–	–	*1.76*	–	–	*0.44*	*0.79*	–	*0.26*	–	–
La	–	–	*20.90*	–	–	*6.29*	*11.60*	–	*12.70*	–	–
Ce	–	–	*42.90*	–	–	*13.50*	*24.50*	–	*30.90*	–	–
Pr	–	–	*5.73*	–	–	*1.90*	*3.44*	–	*4.48*	–	–
Nd	–	–	*24.20*	–	–	*8.83*	*15.40*	–	*21.30*	–	–
Sm	–	–	*4.78*	–	–	*2.05*	*3.59*	–	*4.83*	–	–
Eu	–	–	*1.32*	–	–	*0.65*	*1.16*	–	*1.78*	–	–
Gd	–	–	*4.16*	–	–	*2.03*	*3.50*	–	*5.49*	–	–
Tb	–	–	*0.61*	–	–	*0.30*	*0.53*	–	*0.91*	–	–
Dy	–	–	*3.49*	–	–	*1.69*	*3.04*	–	*5.50*	–	–
Ho	–	–	*0.74*	–	–	*0.34*	*0.65*	–	*1.15*	–	–
Er	–	–	*2.06*	–	–	*0.92*	*1.77*	–	*3.13*	–	–
Tm	–	–	–	–	–	–	–	–	–	–	–
Yb	–	–	*1.96*	–	–	*0.86*	*1.70*	–	*2.79*	–	–
Lu	–	–	*0.30*	–	–	*0.14*	*0.26*	–	*0.41*	–	–

andesites and trachyandesites were provided by Clarke (1990), and we have analysed another five rocks. All are basaltic andesite lavas, ranging from vesicular and formerly glassy, to massive, with plagioclase, augite and rare altered olivine phenocrysts. The Mingelo Volcanics are dominantly a high-K calc-alkaline to shoshonitic suite with strong compositional affinities with the Goonumbla Volcanics basal mafic unit basaltic andesites and with the upper unit of the Fairbridge Volcanics in the Molong Volcanic Belt. This suggests an age around 463–455 Ma (Darriwilian–Gisbornian) and correlation with Phase 2 magmatism.

PARKES–FORBES AREA, EAST OF THE PARKES THRUST

Daroobalgie Volcanics

Small outcrops of andesitic to basaltic lava cropping out just north and east of Forbes have been referred to as the Daroobalgie Volcanics in previous literature (Clarke 1990). They are plagioclase + augite + FeTiox-phyric lavas, and analyses provided by Clarke (1990) suggest that the Daroobalgie Volcanics are shoshonitic, and probably correlatives of the Phase 4 Goonumbla and Wombin Volcanics.

Downloaded by [Auckland University of Technology] at 15:24 09 March 2015

Table 2 Nd and Sr isotopic data for Macquarie Arc igneous rocks.

Sample no.	Lithostratigraphic unit	Age (Ma)	$^{87}Rb/^{86}Sr$	$^{87}Sr/^{86}Sr$ init	$^{147}Sm/^{144}Nd$	ε_{Nd} init
Phase 1						
MB325	**Mitchell Formation andesite clast**	485	0.147	0.70441	0.1354	+7.31
N1	Nelungaloo Volcanics andesite	480	–	–	0.1225	+7.33
N26	Nelungaloo Volcanics basalt	480	–	–	0.1319	+7.48
DR41/94.5	Fairholme Igneous Complex pillow basalt, Boundary	480	–	–	0.1384	+7.57
E43/4/277.6	Cowal Igneous Complex andesite lava, E43	475	–	–	0.1340	+8.15
E42/103/214.5	Cowal Igneous Complex trachyte lava (Golden Lava)	475	–	–	0.1290	+7.79
E42/361/340.6 B	Cowal Igneous Complex trachyte dyke (Golden Lava)	475	–	–	0.1345	+7.90
Phase 2						
1504/60/85.6	Cowal Igneous Complex monzodiorite	465	0.079	0.70390	0.1280	+7.29
E35/1/171.9	Cowal Igneous Complex monzonite	465	0.194	0.70392	0.1506	+8.15
NACD97/53.0	Narromine Igneous Complex Coarse monzogabbro	465	0.083	0.70382	0.1348	+7.39
NACD96/96.0	Narromine Igneous Complex trachytic dyke	465	0.364	0.70396	0.1506	+7.11
E43/2/228.1	Cowal Igneous Complex pl-phyric shallow intr. granodiorite	455	0.187	0.70441	0.1394	+7.67
E43/2/337.2	Cowal Igneous Complex hbd microgabbro	455	0.180	0.70422	0.1479	+7.13
E39/3/195.0	Cowal Igneous Complex high-level granodiorite	455	0.297	0.70397	0.1166	+7.57
ACDMN28/124.9	Cowal Igneous Complex Marsden hbd gabbro	450	0.027	0.70407	0.1356	+7.08
BV5	Parkes Volcanics pl-phyric andesite	465	–	–	0.1354	+7.83
MB115	Cargo Volcanics andesite	465	0.349	0.70486	0.1340	+8.00
MB109	Cargo Volcanics basalt	465	0.180	0.70412	0.1285	+6.98
MB106	Cargo Volcanics dacite lava	465	0.292	0.70444	0.1328	+7.73
WA92	Walli Volcanics aphyric basalt	460	0.154	0.70419	0.1362	+6.97
WA85	Walli Volcanics big plag-phyric andesite	460	0.075	0.70425	0.1327	+6.60
WA99	Walli Volcanics big plag-phyric dolerite dyke	460	0.029	0.70395	0.1408	+6.56
WA40	Walli Volcanics vesicular dacite	460	0.093	0.70432	0.1368	+6.25
PBD52	lower Blayney Volcanics basalt	460	0.184	0.70434	0.1504	+6.31
MB80	upper Blayney Volcanics basalt	455	0.167	0.70400	0.1697	+7.20
KA31	Fairbridge Volcanics basal ol+cpx-phyric basalt	455	0.014	0.70435	0.1480	+6.77
MB145	Fairbridge Volcanics Unit 4 strongly pl-phyric basalt	450	0.041	0.70420	0.1452	+5.58
RDW2	Byng Volcanics cumulate ol-rich wehrlite	455	0.009	0.70445	0.1753	+6.85
RDW80	Byng Volcanics primitive ol+cpx-phyric basalt	455	0.145	0.70491	0.1653	+6.50
RDW142	Byng Volcanics primitive ol+cpx-phyric basalt	455	0.412	0.70371	0.1676	+6.53
RDW193	Byng Volcanics basalt	455	0.033	0.70451	0.1690	+6.96
BLRS0479	Mt Pleasant Basalt Member, Forest River Volcanics	455	–	–	0.1355	+7.65
Phase 3						
NACD83/148.4	Narromine Igneous Complex Copper Hill-type dacite	448	0.117	0.70379	0.1206	+6.43
NACD86/129.4	Narromine Igneous Complex Copper Hill-type granodiorite	448	0.081	0.70385	0.1185	+6.93
MB130	Copper Hill qtz diorite intrusive	448	–	–	0.1125	+7.40
MB143	Copper Hill dacitic intrusive	448	–	–	0.1287	+6.72
Phase 4						
MB50	Ferndale Monzonite (central Molong Belt)	445	0.129	0.70412	0.1280	+6.80
BLRS0619	Glen Ayr syenite (central Molong Belt)	445	–	–	0.1161	+6.73
CSG88	Goonumbla Volcanics basal mafic unit	445	–	–	0.1325	+6.04
CSG114	Goonumbla Volcanics trachyandesite	445	–	–	0.1410	+5.96
10/22/12	Wombin Volcanics pl-bi-phyric trachyte	445	–	–	0.1269	+5.77
WA31	Angullong Formation andesite	440	0.054	0.70442	0.1471	+5.49
WA27	Angullong Formation basaltic andesite	440	0.141	0.70477	0.1485	+4.94
MB99	Millthorpe Volcanics evolved basalt	445	0.124	0.70464	0.1462	+6.75
PBD42	Millthorpe Volcanics evolved basalt	445	0.159	0.70388	0.1429	+6.20
KA82	Cheesemans Creek Formation big plag basalt lava	445	0.148	0.70433	0.1202	+6.04
DR34/150.9	Fairholme Igneous Complex hbd-phyric intrusive, Boundary	440	–	–	0.1391	+6.29
MORS0120	Forest Reefs Volcanics, dioritic intrusive	440	–	–	0.1215	+6.37

(*continued*)

Downloaded by [Auckland University of Technology] at 15:24 09 March 2015

Table 2 (*Continued*).

Sample no.	Lithostratigraphic unit	Age (Ma)	$^{87}Rb/^{86}Sr$	$^{87}Sr/^{86}Sr$ init	$^{147}Sm/^{144}Nd$	ε_{Nd} init
E37/3/245.2	Zero porphyry, trachyte, Northparkes	437	–	–	0.1174	+4.98
BV1	Bushman Volcanics hbd+pl+cpx-phyric andesite	436	–	–	0.1077	+4.72
NH21	Nash Hill Volcanics pl+cpx+hbd-phyric basalt	436	–	–	0.1006	+2.07
NH19	Nash Hill Volcanics strongly cpx-phyric basalt	436	–	–	0.1151	+3.54
NH15	Nash Hill Volcanics pl+hbd-phyric andesite	436	–	–	0.1042	+2.93
NH18	Nash Hill Volcanics pl+cpx+hbd andesite	436	–	–	0.1029	+2.63

Parkes Volcanics

Four volcanic units have been recognised (Krynen *et al.* 1990; Lyons *et al.* 2000; this study) as elongate north-northeast-oriented, fault-bounded slivers of volcanic rocks in a high-strain zone that extends for about 15 km eastward from the Parkes Thrust (Figure 4). From east to west, these are the Nash Hill Volcanics, the Bushman Volcanics, and the Parkes Volcanics; the fourth unit, the Goobang Volcanics, occurs as a poorly exposed sliver not sampled for this study. Based on geochemical data from this study, correlations and sparse age dating, the Nash Hill Volcanics and the Bushman Volcanics are interpreted to be Early Silurian units (see below), whereas we link the Parkes Volcanics to Middle Ordovician Phase 2 magmatism.

The Parkes Volcanics occur in the westernmost of the three narrow, elongate volcanic belts east of the Parkes Thrust (Figure 4) (Glen *et al.* 2007b) and have a relatively limited distribution in terms of both aeromagnetic definition and actual outcrop. They occur immediately along the western side of Parkes township and extend ~3 km north of Parkes and 5 km south, with a maximum apparent width of ~2 km. The Parkes Volcanics are moderately plagioclase-phyric basaltic andesites and andesites with subordinate augite phenocrysts, but no apatite microphenocrysts; they lack phenocrystic hornblende and are moderately foliated in proximity to the Parkes Thrust. A single shallow intrusive microgranodioritic dyke rock (BV6 in Table 1) intruding andesites of the Parkes Volcanics contains plagioclase, quartz and K-feldspar phenocrysts in a holocrystalline, sugary groundmass. This unit has the diagnostic high Nb geochemical signature of the Lower Silurian Nash Hill Volcanics (see below).

The Parkes Volcanics are compositionally distinct from both the Nelungaloo Volcanics and the Goonumbla and Wombin Volcanics. This is effectively shown by the consistently higher TiO_2 contents and the distinctively high, fractionation-unaffected Zr/Nb values (28–38) of the Parkes Volcanics (Figure 5a). Among Macquarie Arc Ordovician lavas, only the Cargo and Walli Volcanics, and some lavas from the lower parts of the Fairbridge Volcanics, all in the Molong Volcanic Belt, show this same high Zr/Nb range (Figure 5a). Although the Parkes Volcanics have TiO_2 contents higher than either the Cargo or Walli Volcanics (Figure 5a), the distinctive high Zr/Nb and other key immobile element abundances and ratios all support broad correlation of the Parkes Volcanics with the Cargo and Walli Volcanics. All formerly glassy porphyritic Cargo, Walli and Parkes Volcanics lavas have suffered some degree of K_2O depletion as suggested by the Al_2O_3-normalised K_2O and P_2O_5 contents (Figure 5b), and this plot and $MgO-P_2O_5$ relationships (Figure 5c) indicate high-K calc-alkaline or shoshonitic affinities for the Parkes Volcanics lavas. The Parkes Volcanics have REE patterns (Figure 5d) and a distinctively high ε_{Nd} value (+7.83) within the range for Cargo and Walli Volcanics (+6.6 to +8.0 for six samples: Simpson *et al.* 2007) (Table 2).

Thus, available data suggest that the Parkes Volcanics are likely to be contemporaneous with the Cargo and Walli Volcanics package. This supports the suggestion based on seismic-reflection profiles (Glen *et al.* 1998, 2004a; Direen *et al.* 2001) that similar lavas may underlie large parts of the Cowra Trough.

Bushman Volcanics and Nash Hill Volcanics

East of the Parkes Volcanics is a series of fault slices dominated by lavas and lava breccias of mainly andesitic composition that have been previously assigned to two separate units, the Bushman Volcanics and the Nash Hill Volcanics (Figure 4). The latter extend southwest towards Forbes. They structurally, and probably conformably, interfinger with the Lower Silurian Cotton Formation, and thus post-date the major magmatic expression of the Macquarie Arc. They may be better correlated with shoshonitic magmas that formed the Alaskan-type Fifield complexes in the Early Silurian (see below). The obvious fault-controlled linear nature of the aeromagnetic expression of these volcanic belts, and poor outcrop, have prevented unambiguous interpretation of the relationships between adjacent volcanic units, although the occurrence of undoubted Bushman-type andesites in the westernmost section of what was mapped as the Nash Hill Volcanics (around 610850–611300E, 633400–633470N, just northeast of Parkes) suggests an interfingering relationship between the two units. The Nash Hill Volcanics are notable for their particularly strong and distinctive Th signal on the regional radiometrics (Lyons *et al.* 2000), over areas of outcrop. The best-defined section of the Bushman Volcanics crops out over a relatively restricted area north of and in Parkes township as small elongate outcrop zones, and as slices in Silurian Forbes Group sedimentary rocks just further north.

Downloaded by [Auckland University of Technology] at 15:24 09 March 2015

Downloaded by [Auckland University of Technology] at 15:24 09 March 2015

The Bushman Volcanics andesite lavas and lava breccias have common phenocrystal hornblende and apatite, along with plagioclase, sparse augite, and FeTi oxides. The Nash Hill Volcanics are mainly coherent to autobrecciated lavas, pillowed in places, which vary compositionally from basalt to andesite. The more mafic lavas are strongly augite-phyric vesicular basalts with subordinate and smaller plagioclase phenocrysts, and sparse altered olivine phenocrysts. More evolved Nash Hill Volcanics lavas also commonly have hornblende phenocrysts.

Geochemically, both the Bushman Volcanics and the Nash Hill Volcanics contain two quite distinct compositional suites (Table 1) based largely on P_2O_5 contents (Figures 6a, 7a). Both suites in the Bushman Volcanics are compositionally distinct from the Goonumbla and Wombin volcanic suites, and from the nearby Parkes Volcanics, because of their very low TiO_2 contents ($<0.5\%$; Figure 6b). The Bushman Volcanics lavas with lower P_2O_5 have Al-normalised P_2O_5–K_2O relationships (Figure 6a) suggesting medium-K calc-alkaline affinities, whereas the volumetrically dominant higher P_2O_5 group are clearly shoshonitic. REE patterns for Bushman Volcanics higher P_2O_5 trachyandesites (Figure 6c) show greater LREE enrichment than the Goonumbla and Wombin Volcanics shoshonitic trachyandesites. A higher P_2O_5 Bushman Volcanics andesite has an age-corrected ε_{Nd} value of +4.72 (Table 2), significantly lower than any sample of Goonumbla or Wombin Volcanics.

The lower P_2O_5 (0.22–0.36%) group basalts and andesites in the Nash Hill Volcanics have transitional high-K calc-alkaline to shoshonitic affinities (Figure 6a), whereas the higher P_2O_5 Nash Hill Volcanics are compositionally distinctive shoshonitic lavas with strikingly high Nb, LREE and Th contents (20–35 ppm) and extremely low Zr/Nb values (Table 1; Figures 6b, 7a). The REE patterns of Nash Hill Volcanics are broadly parallel and show significantly higher LREE enrichment than those for the shoshonitic Goonumbla and Wombin Volcanics (Figure 6c). New ε_{Nd} values for four Nash Hill Volcanics are lower than for the Macquarie Arc lavas and define a general mixing line (Figure 7b, c) between a strongly Th- and LREE-enriched component with high Nb and P_2O_5 ($\sim$40 ppm and 0.7% minimum values, respectively) contents and ε_{Nd} close to, or less than, 0, and a component close to the field for Goonumbla and Wombin Volcanics. The strongly enriched low Zr/Nb, low ε_{Nd} component is unlikely to be a crustal component, as a feature of the continental crust is significant depletion in Nb ($\sim$10 ppm). MORB-normalised multi-element patterns (Figure 7d) for the two most enriched Nash Hill Volcanics show Th, U, Pb, Sr and La–Ce abundances too high for the enriched component to be an average intraplate basalt (e.g. OIB), even if it were contaminated by typical continental crust (since the pattern for the latter is below the average OIB for all elements plotted). The mantle-derived component involved was significantly more enriched in these elements than typical intraplate basalts, and may have been more lamprophyric in composition.

COWAL AND FAIRHOLME IGNEOUS COMPLEXES

The Cowal (eastern) and Fairholme (western) Igneous Complexes are two aeromagnetically defined large areas of Ordovician volcanic–volcaniclastic rocks at the southwest end of the Junee–Narromine Volcanic Belt, juxtaposed against the Booberoi Shear Zone. These rocks are described in more detail in Glen *et al.* (2007b) and Crawford *et al.* (2007).

Interpretation of aeromagnetic data ground-truthed by aircore sampling suggests that in the Cowal Complex, inferred Early Ordovician Phase 1 lavas are intruded by numerous medium to small, Middle to Late Ordovician stocks that range petrographically from monzogabbros, monzodiorites and monzogranites to hornblende gabbros, diorites, granodiorites and high-level granophyric felsic intrusive rocks. These intrusive rocks include representatives of both Phase 2 and Phase 3 magmatism. Considerably more work is required to clarify relationships between these intrusive rocks. For example, even for available data from the Muddy Lake Gabbro around the Cowal deposit (E42), holocrystalline diorites with 53–60% SiO_2 show TiO_2 contents that cluster in two separate groups, and include high-K_2O calc-alkaline compositions among those fresh rocks with lower SiO_2 contents, whereas the fresh rocks with 56–67% SiO_2 all have medium-K affinities. An Ar/Ar age of 465.7 ± 1 Ma was reported for an E42 intrusive rock by Miles and Brooker (1998), whereas Crawford *et al.* (2007) suggest that most holocrystalline intrusive rocks encountered in shallow drilling in the Cowal Igneous Complex are best classified as medium-K calc-alkaline diorites and (I-type) granodiorites, sometimes associated with more mafic hornblende gabbros, and that they represent Phase 3 magmatism (455–445 Ma). The latter differ from the Phase 4 shoshonitic porphyries in the Northparkes Group, and from correlated intrusions in the Molong Volcanic Belt, by having more quartz, more hornblende, less biotite and less K-feldspar.

In the Fairholme Igneous Complex, basaltic lavas probably associated with Early Ordovician Phase 1 magmatism are intruded by stocks and sheets best correlated with Late Ordovician Phase 4 high-K calc-alkaline and shoshonitic magmatism (Crawford *et al.* 2007).

NARROMINE IGNEOUS COMPLEX

The Narromine Igneous Complex consists of unexposed, probably Early Ordovician basaltic and andesitic volcanics and volcaniclastic sedimentary rocks intruded by large *ca* 465 Ma (Phase 2) plutons that vary from monzogabbro to monzonite compositions, and a later (450–445 Ma) suite of comagmatic holocrystalline medium-K calc-alkaline granodiorites and porphyritic intrusive dacites assigned to Phase 3 magmatism (Crawford *et al.* 2007).

MOLONG VOLCANIC BELT

The Molong Volcanic Belt consists of two main regional domains that include both Middle and Late Ordovician volcanic rocks. These are the Cargo block on the

Downloaded by [Auckland University of Technology] at 15:24 09 March 2015

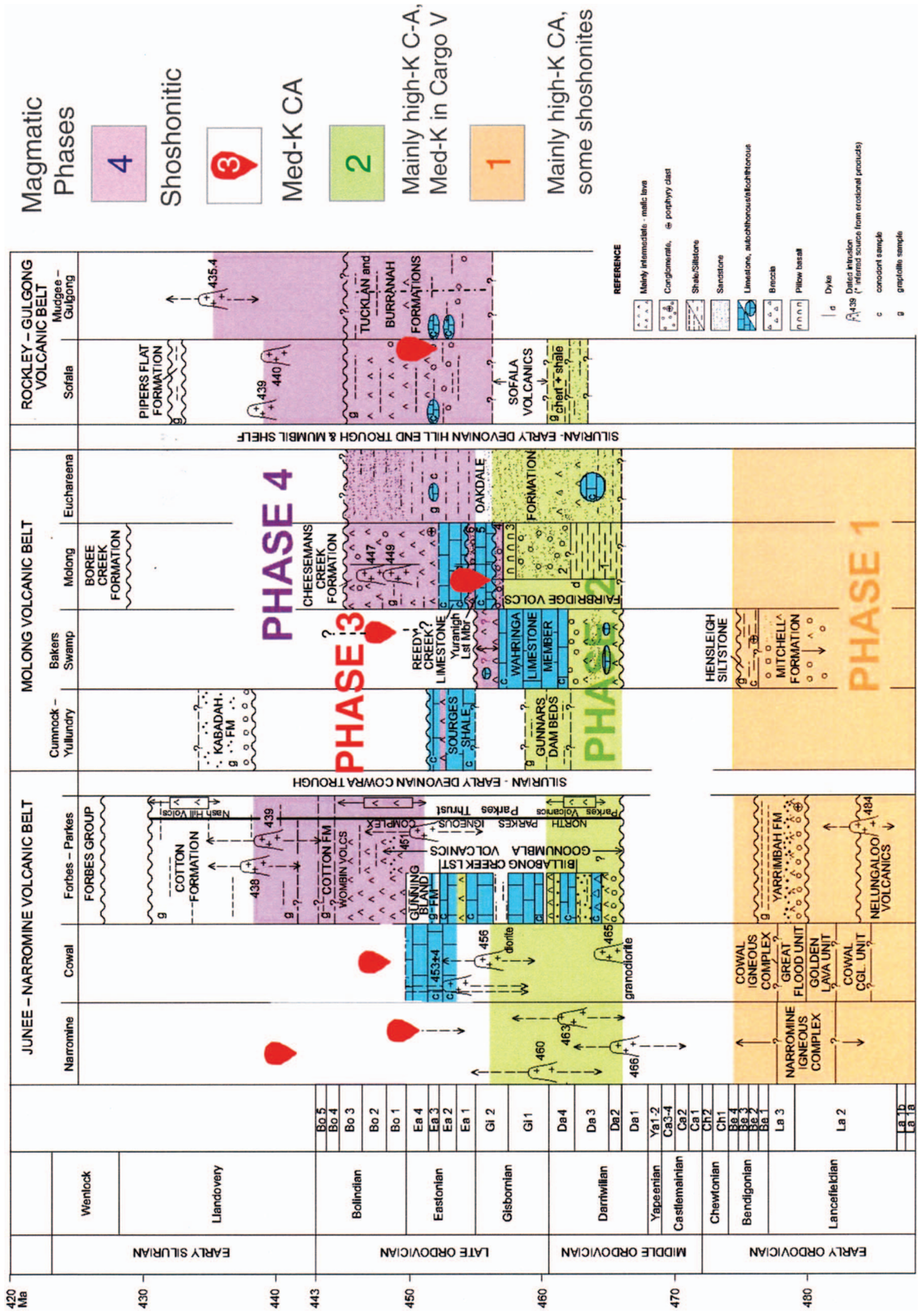

Figure 2 (*Continued*).

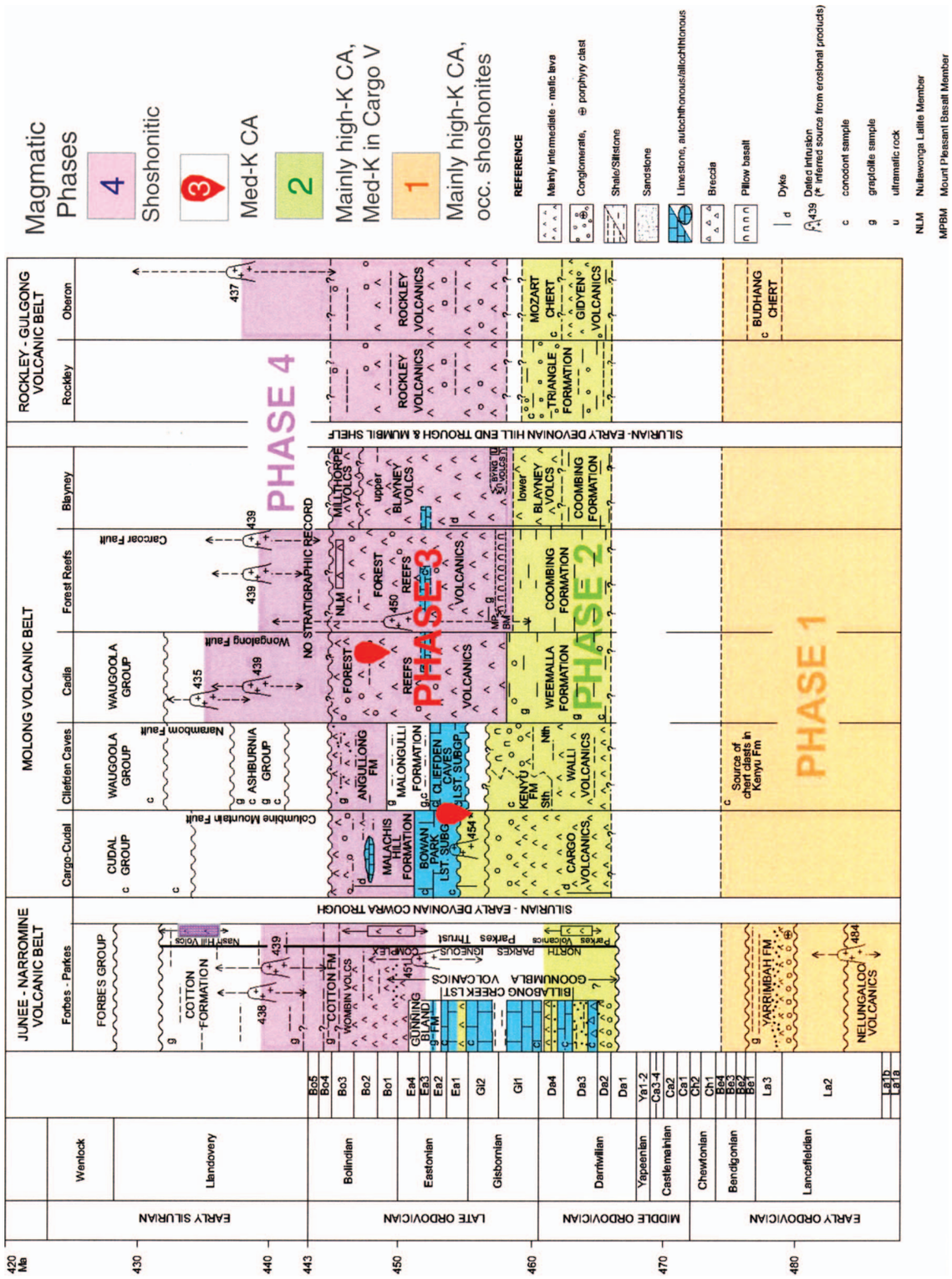

Figure 2 Lithostratigraphic column for the Macquarie Arc colour-coded to show magmatic affinities of the major lithostratigraphic units, and showing Magmatic Phases 1–4 in the Ordovician history of the arc (age relationships from Percival & Glen 2007).

Downloaded by [Auckland University of Technology] at 15:24 09 March 2015

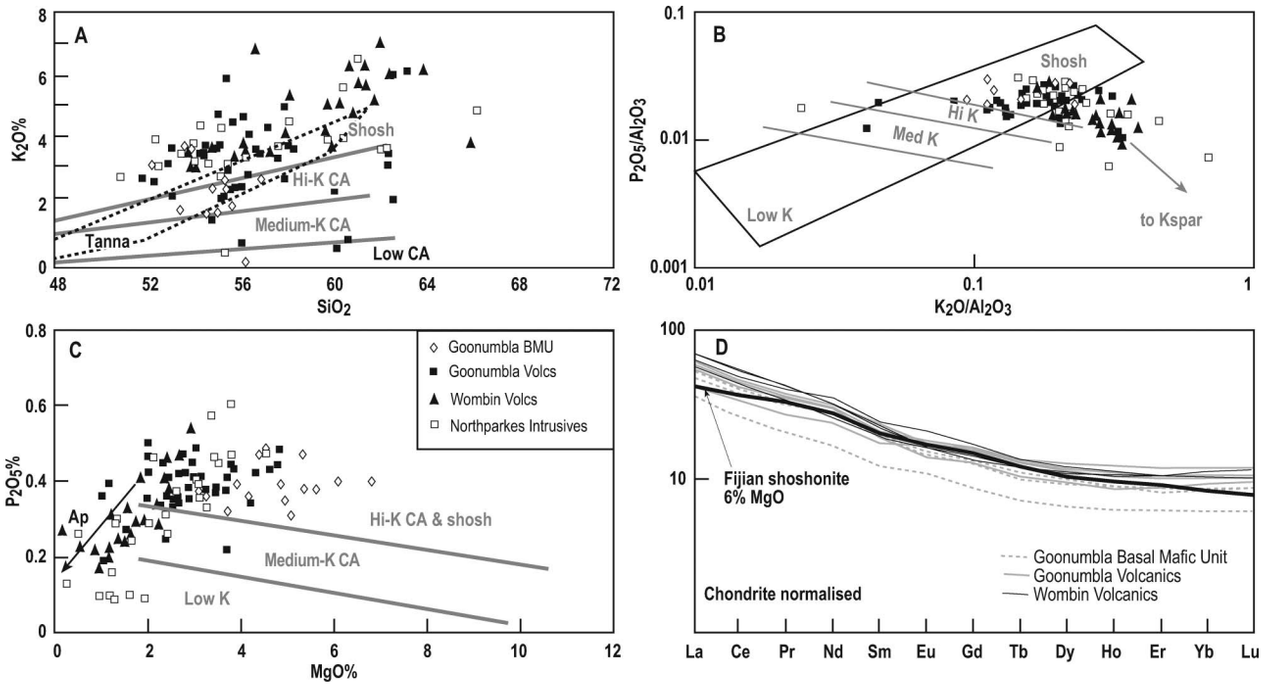

Figure 3 (a) K_2O *vs* SiO_2 showing Goonumbla basal mafic unit, Goonumbla and Wombin Volcanics, intrusives, and lavas from Tanna island (Vanuatu arc). (b) K_2O/Al_2O_3 *vs* P_2O_5/Al_2O_3 for the units shown in (a), with compositional field and boundaries for modern lavas from the Vanuatu and Sunda arcs; lavas plotting to the left of the field have lost K_2O during alteration of largely glassy groundmasses. (c) P_2O_5 *vs* MgO for the units shown in (a), with vector showing effect of fractionation involving apatite, and compositional field boundaries defined by modern lavas from the Vanuatu and Sunda arcs. (d) Chondrite-normalised REE patterns (normalising values from Boynton 1984) for lavas from the Goonumbla and Wombin Volcanics and a typical Fijian shoshonite with 6% MgO shown for comparison (Rogers & Setterfield 1994).

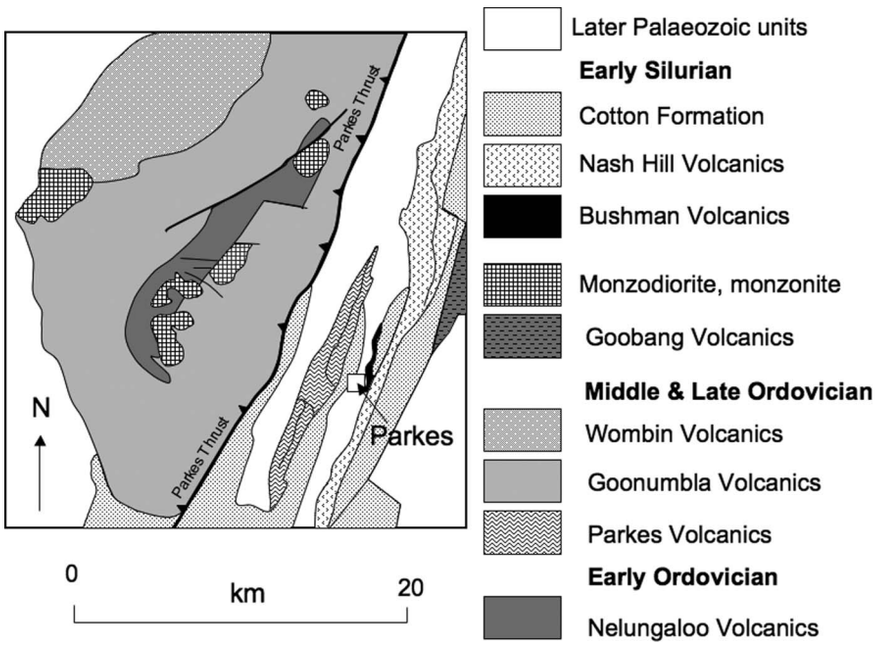

Figure 4 Simplified geological map of the area around Parkes in the Junee–Narromine Volcanic Belt showing the Parkes Thrust and the major volcanic units to the east of this structure, including the Parkes, Bushman and Nash Hill Volcanics (after Glen *et al.* 2004a).

western side of the volcanic belt, and the main, meridional, essentially continuous volcano-sedimentary packages extending between Wellington in the north and Blayney in the south (Figure 1). The geology and geochemistry of the Cargo block are described in detail in Simpson *et al.* (2007), and the Forest Reefs–Neville region at the southern end of the Molong Belt is described in Squire and Crawford (2007) and Squire and McPhie (2007).

Downloaded by [Auckland University of Technology] at 15:24 09 March 2015

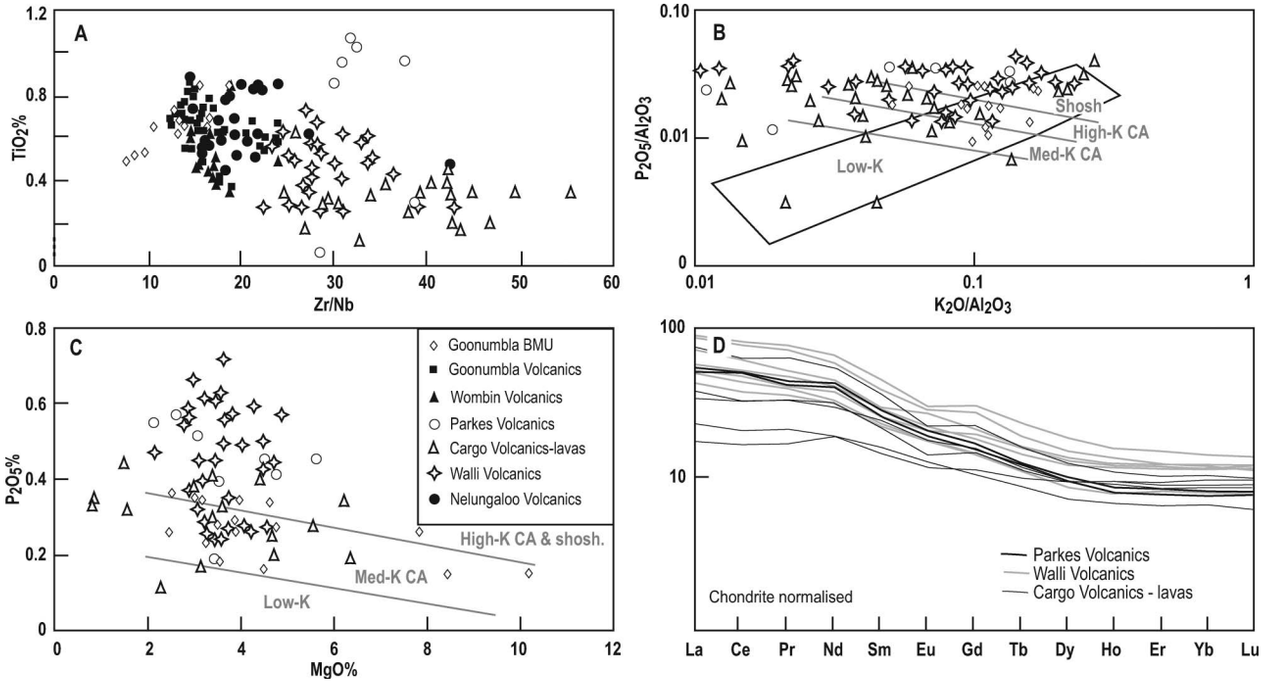

Figure 5 (a) Zr/Nb *vs* TiO_2 for Middle and Late Ordovician volcanic units in the Junee–Narromine Volcanic Belt and the Cargo block of the Molong Volcanic Belt, emphasising the high Zr/Nb values that characterise the Cargo, Walli and Parkes Volcanics. (b) K_2O/Al_2O_3 *vs* P_2O_5/Al_2O_3 for the units shown in (a). (c) P_2O_5 *vs* MgO for the units shown in (a). (d) Chondrite-normalised REE patterns (normalising values from Boynton 1984) for lavas from the Parkes, Walli and Cargo Volcanics, emphasising the similarity of the patterns for these Middle Ordovician units.

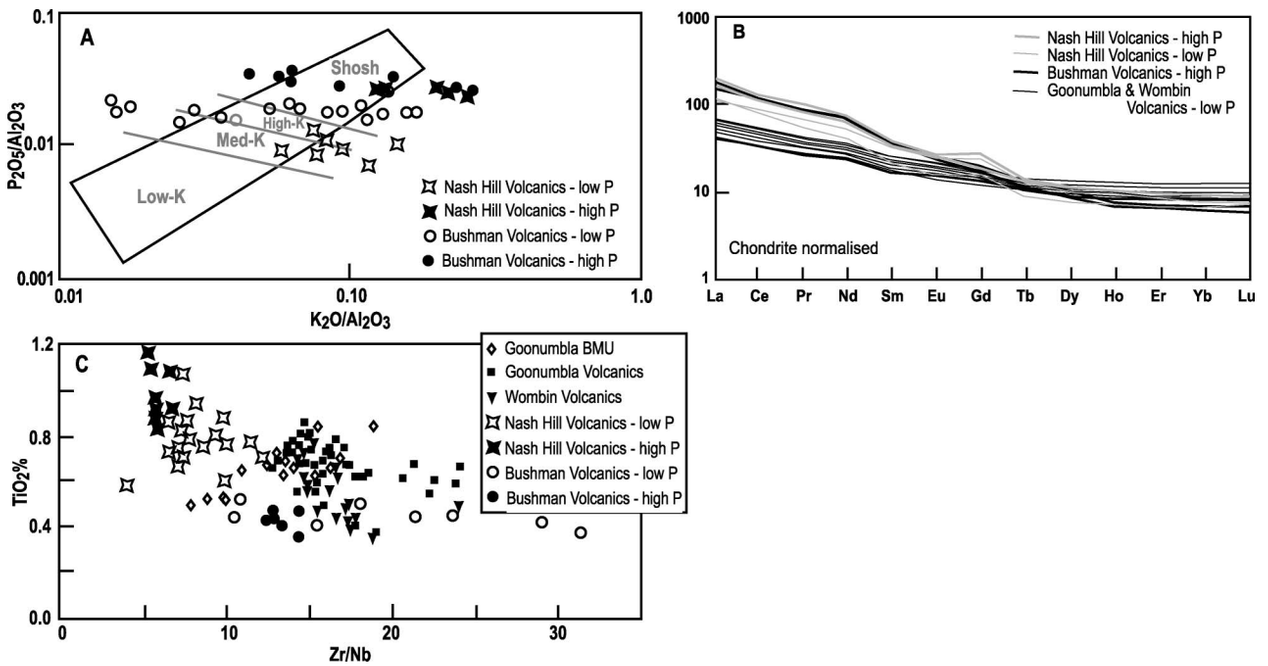

Figure 6 (a) K_2O/Al_2O_3 *vs* P_2O_5/Al_2O_3 for the Bushman and Nash Hill Volcanics showing that both units include a higher P_2O_5 and a lower P_2O_5 compositional group. (b) TiO_2 *vs* Zr/Nb for the Bushman and Nash Hill Volcanics comparing them with lavas from the Goonumbla and Wombin Volcanics. Note the strikingly low Zr/Nb values for the Nash Hill Volcanics. (c) Chondrite-normalised REE patterns (normalising values from Boynton 1984) for the Bushman and Nash Hill Volcanics comparing them with lavas from the Goonumbla and Wombin Volcanics.

Downloaded by [Auckland University of Technology] at 15:24 09 March 2015

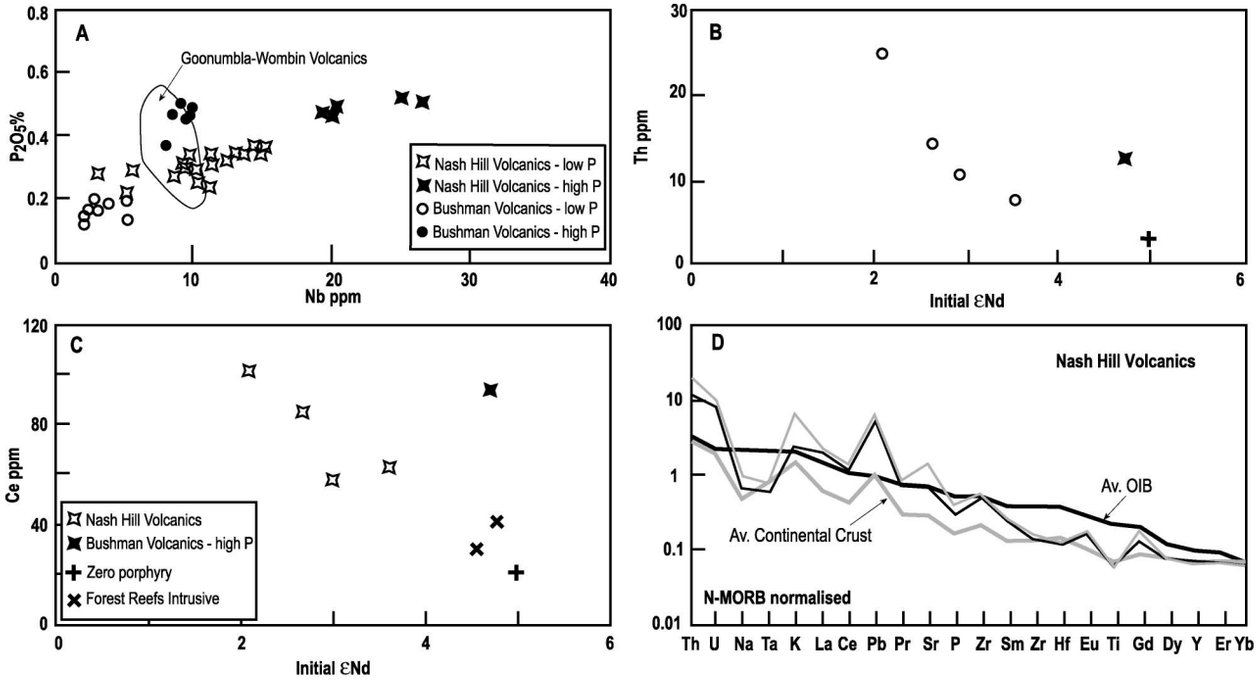

Figure 7 (a) P_2O_5 *vs* Nb for Bushman and Nash Hill Volcanics showing a straight-line relationship inferred to represent mixing between a high-Nb, high-P end-member and a low-P, low-Nb end-member. (b) Th and (c) Ce *vs* initial ε_{Nd} for Bushman Volcanics, Nash Hill Volcanics and the zero porphyry trachyte unit of the Wombin Volcanics, one of the youngest volcanic rocks in the main section of the Junee–Narromine Volcanic Belt. The curved relationship supports mixing between a high-Th, high-Ce, low ε_{Nd} component and a low-Ce, low-Th, high ε_{Nd} component (see text for discussion). (d) N-MORB-normalised multi-element patterns (normalising values from Sun & McDonough 1989) for two high-P Nash Hill Volcanics basaltic lavas compared with an average ocean island intraplate basalt (OIB), and an average continental crust composition (from Taylor & McLennan 1985). The enriched component involved in the production of the Nash Hill Volcanics was considerably enriched in Th, U, P and Sr, and depleted in high-field-strength elements (Nb, Ta, Zr, Hf, Ti) relative to the average OIB.

Cargo block

CARGO AREA

The Cargo region contains a thick pile of lavas and volcaniclastic rocks believed to be erupted in a Middle Ordovician intra-oceanic arc volcano, overlain by the Eastonian Bowan Park Limestone Subgroup. Simpson *et al.* (2007) provide a detailed study of the Cargo Volcanics. Here, we summarise relevant geochemical data from Cargo and the adjacent Walli areas.

The Cargo Volcanics are a dominantly basaltic andesite sequence with subordinate evolved andesites and more felsic lavas and pumice breccias that pass up into volcaniclastic sediments. All lavas have fractionation-independent Zr/Nb values between 25 and 50, in strong contrast to most other Molong Volcanic Belt lavas which have Zr/Nb <20 (Figure 5a). Apart from the Parkes Volcanics (see above), only the Walli Volcanics, and some of the Fairbridge Volcanics from the Molong area, show these high Zr/Nb values. However, in the Cargo block, no lavas with $>6\%$ MgO are recorded. In contrast, the Fairbridge lavas in the Molong area include quite primitive clinopyroxene-rich ankaramites, often with MgO $>6\%$ (Table 1). Alteration (quartz–chlorite–albite) of the commonly formerly glassy Cargo Volcanics lavas precludes their meaningful classification on the basis of K_2O-SiO_2 relationships, but Al-normalised $P_2O_5-K_2O$ (Figure 5b), P_2O_5–MgO relationships (Figure 5c) and REE patterns (Figure 5d) suggest affinities with medium- to high-K calc-alkaline lavas (Simpson *et al.* 2007). Many dykes in the Cargo Volcanics show similar high Zr/Nb and $MgO-P_2O_5$ relationships to the host lavas and probably represent feeders to these lavas, but dykes with higher P_2O_5 contents and lower Zr/Nb are not uncommon in the Cargo block. Some dykes are compositionally very close to the Walli Volcanics, and in the northern end of the block, coarsely plagioclase-phyric basaltic andesite dykes are petrographically and geochemically identical to Phase 4 Malachis Hill Formation lavas overlying the Bowan Park Limestone Subgroup (Figure 1) (Simpson *et al.* 2007). New ε_{Nd} data for the Cargo Volcanics (+6.9 to +7.8: Table 2) show the highest values recorded in our study of the Molong Volcanic Belt and indicate minimal involvement of old crust in the petrogenesis of the Cargo Volcanics, being close to those for 450 Ma depleted upper mantle.

The volcanic facies architecture of the Cargo Volcanics suggests that they formed the core zone of a growing marine stratovolcano (Simpson *et al.* 2007) flanked by a proximal volcaniclastic apron of resedimented debris. The absence of lavas with MgO $>6\%$ also suggests storage and eruption in a major arc volcano plumbing system compared with similar lavas farther north in the Molong Volcanic Belt that presumably

Downloaded by [Auckland University of Technology] at 15:24 09 March 2015

Downloaded by [Auckland University of Technology] at 15:24 09 March 2015

bypassed major storage chambers away from the main volcanic edifice. Well-rounded clasts in the upper part of the succession, together with large volumes of unabraded crystal detritus and lithic fragments, suggests shoaling of the volcano to shallow water or subaerial conditions. Detrital quartz is absent in most volcaniclastic sediments apart from those immediately below the Bowan Park Limestones and those in the basal Ranch Member of the Bowan Park Limestone Subgroup (Packham *et al.* 2003), where the quartz occurs together with detrital hornblende. Laser ablation ICP-MS dating of detrital zircons in one of these sandstones gives an age of 453 ± 5 Ma (Simpson *et al.* 2007), suggesting that the detrital quartz, hornblende and zircons may have been derived from recently emplaced and exposed Phase 3 Copper Hill-type dacitic intrusions.

Several small unmineralised monzodiorite–monzonite bodies transect Phase 3 intrusive dacites at Cargo and show shoshonitic affinities (Simpson *et al.* 2007). These monzonitic intrusions are undated, but may correlate with those near Cadia, dated at 439 ± 1 Ma (Perkins *et al.* 1990, 1992). A later swarm of pink Ti-augite-bearing transitional alkaline basaltic and doleritic dykes intrudes all other igneous rocks in the Cargo block, and matches those in the Cowal and Fairholme Igneous Complexes, and further north around Molong in the Molong Volcanic Belt.

Above the Bowan Park Limestone Subgroup in the Malachis Hill area at the northern end of the Cargo block is the Malachis Hill Formation, a sequence of well-bedded, planar-laminated turbiditic black siltstones at least 350 m thick (Percival & Glen 2007; Simpson *et al.* 2007) that contains lenses of strongly plagioclase-phyric pillowed shoshonitic basalt. This sequence coarsens upward into crystal-lithic sandstones and an overlying conglomerate at least 300 m thick that contains a polymictic assemblage of rounded and subrounded clasts dominated by clinopyroxene-rich shoshonitic basaltic andesites that are locally derived, and Late Ordovician post-limestone in age. Clasts have Zr/Nb values that rule out a source from either the Cargo or Walli Volcanics. Overlying the conglomerate is a coral-bearing, possibly allochthonous limestone of late Bolindian age (Percival & Glen 2007). A Malachis Hill Formation basalt has an ε_{Nd} value of +6.0: Table 2), within the range for Phase 4 shoshonites from the Molong Volcanic Belt.

WALLI–CLIEFDEN CAVES AREA

The Walli Volcanics, southeast of the Cargo block, are dominated by distinctive 'big-plagioclase basalts', although sparsely plagioclase + clinopyroxene-phyric and aphyric lavas are also present. The occurrence of several dykes with 'Walli' compositions within the Cargo Volcanics (Simpson *et al.* 2007) suggests that the Walli magmatism slightly post-dates Cargo Volcanics magmatism. Unlike in the Cargo block, no dacitic lavas are recorded, and basalts and basaltic andesites dominate most exposed sections. Geochemically, the Walli Volcanics show high-K calc-alkaline to shoshonitic affinities, with generally higher P_2O_5 (and presumably originally, higher K_2O) contents than the Cargo Volcanics (Figure 5b, c). The Walli Volcanics share the same high Zr/Nb values (20–50) as the Cargo Volcanics (Figure 5a), which effectively separates them from the other Middle and Late Ordovician volcanic suites occurring farther east. Four Walli lavas ranging from basalt to dacite have ε_{Nd} values ranging from +6.1 to +7.0 (Table 2). The lower ε_{Nd} values are in keeping with the higher K_2O, higher P_2O_5 values for the Walli Volcanics compared with the Cargo Volcanics. A temporal change to higher P_2O_5 and K_2O, and lower ε_{Nd} is indicated.

In the Cliefden Caves area, limestones of the Cliefden Caves Limestone Subgroup (Percival & Glen 2007) are overlain by the late Eastonian to earliest Bolindian Malongulli Formation, mainly composed of siltstones of deep-water aspect and very similar to the Malachis Hill Formation sediments above the Bowan Park Limestone Subgroup (see below, and Simpson *et al.* 2007), followed upward by the Angullong Formation. Lavas in the Bolindian Phase 4 Angullong Formation are petrographically distinctive plagioclase + hornblende + augite + FeTiox + apatite-phyric andesites, and they have clear shoshonitic compositions (Table 1; Figure 8a, b). New ε_{Nd} isotopic data (Table 2) for Angullong lavas show lower values (+4.9 to +5.6) than the Cargo and Walli Volcanics, and match other post-Eastonian shoshonitic volcanics in both the Junee–Narromine and Molong volcanic belts.

Northern Molong Volcanic Belt

The northern section of the Molong Volcanic Belt extends northwards from under the Tertiary Canobolas Complex near Orange, to the Bodangora area ~10 km north of Wellington, where Ordovician rocks disappear beneath younger cover. This part of the Molong Volcanic Belt has been broadly subdivided (Pogson & Watkins 1998) into the volcaniclastic-dominated Oakdale Formation and the Fairbridge Volcanics. However, significant complexities exist in that at least one section of the stratigraphy currently mapped (Pogson & Watkins 1998) as Oakdale Formation is almost certainly better correlated with the Fairbridge Volcanics. Around Molong in the southern part of this belt, Fairbridge Volcanics overlie Eastonian limestones that pass up into Phase 4 shoshonitic lavas of the Cheesemans Creek Formation (Scott *et al.* 1998).

EARLY ORDOVICIAN TO MIDDLE ORDOVICIAN TRANSITION

The boundary between the Lower Ordovician Hensleigh Siltstone and the Middle Ordovician Wahringa Limestone and Fairbridge Volcanics is poorly exposed (Percival & Glen 2007). An unconformity is suspected on the basis of the large (~9 million years) time break between the fossil-dated sequences, although a genuine erosional hiatus (i.e. unconformity) has not been found. In the Wahringa area ~25 km south of Wellington, the basal part of the Fairbridge Volcanics below the 88 m thick late Darriwilian–late Gisbornian Wahringa Limestone Member includes common cobble conglomerates and coarse lava breccias dominated by

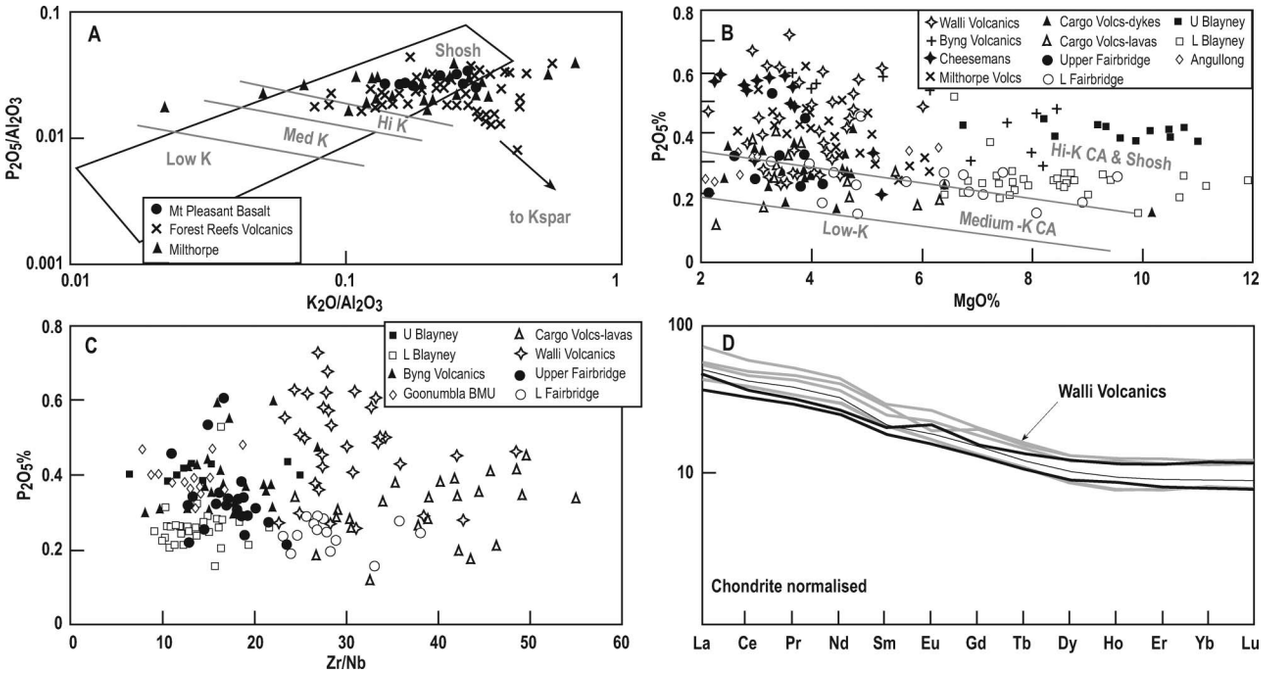

Figure 8 (a) K_2O/Al_2O_3 *vs* P_2O_5/Al_2O_3 for shoshonitic Phase 4 magmatic suites from the Molong Volcanic Belt, including Cheesemans Creek Formation, Angullong Formation, Forest Reefs Volcanics, Millthorpe Volcanics and Mt Pleasant Basalt Member of the Forest Reefs Volcanics. (b) P_2O_5 *vs* MgO for Phase 4 shoshonitic suites (Angullong Formation, Cheesemans Creek Formation, Millthorpe Volcanics) and Phase 2 volcanic lithostratigraphic units in the Molong Volcanic Belt (Fairbridge Volcanics, Cargo Volcanics, Walli Volcanics, Byng Volcanics). (c) Zr/Nb *vs* P_2O_5 for Phase 2 volcanic-dominated lithostratigraphic units in the Molong Volcanic Belt, and for the basal mafic unit of the Goonumbla Volcanics in the Junee–Narromine Volcanic Belt. (d) Chondrite-normalised REE patterns (normalising values from Boynton 1984) for lower Fairbridge Volcanics lavas, showing patterns for Walli Volcanics from the Cargo block for comparison.

plagioclase-phyric low-MgO andesites and dacites (Percival & Glen 2007). Similar lavas and volcaniclastics occur immediately above the Wahringa Limestone Member, but they tend to be more mafic up-sequence, with basalts and basaltic andesites occurring <70 m above the main limestone.

FAIRBRIDGE VOLCANICS AND OAKDALE FORMATION

The Fairbridge Volcanics range from Darriwilian Da2 (*ca* 465 Ma) to latest Gisbornian (*ca* 455 Ma) in age (Figure 2) and represent Phase 2 magmatism. They consist of a west-dipping and west-younging packet of volcanic and volcano-sedimentary rocks 40 km long and up to 8 km wide, with a true stratigraphic thickness of <2 km. Included in the Fairbridge Volcanics are a number of discrete *in situ* and allochthonous limestones, including the late Darriwilian–late Gisbornian Wahringa Limestone Member, and the late Gisbornian Yuranigh Limestone Member (Figure 2). The Fairbridge Volcanics are overlain by the early Eastonian Reedy Creek Limestone (Percival & Glen 2007). Based on the best exposed outcrops around Molong (Figure 9), we have subdivided the Fairbridge Volcanics into six units based on volcanic facies and petrography. These are described below from the base to the top.

Unit 1 is $\sim$500–1000 m thick (base not exposed) and dominated by volcaniclastic sandstones and siltstones with minor conglomerate, sills and dykes. Unlike overlying Unit 2 volcaniclastic sandstones, these sandstones are dominated by andesitic clasts and commonly contain quartz-bearing intrusive clasts ($\sim$5–10%), many with distinctive granophyric intergrowths of quartz and plagioclase. This unit was previously mapped as part of the Oakdale Formation (Pogson & Watkins 1998). However, it contains distinctly different clast types to the Oakdale Formation, and lies conformably beneath the main package of Fairbridge Volcanics. Aeromagnetic images and our mapping show no obvious faults separating these rocks from the Fairbridge Volcanics, and in the field these rocks increase in grainsize until they become an indistinguishable part of the rocks previously mapped as Fairbridge Volcanics. Dykes are common throughout this unit, and their geochemical affinities suggest that most are feeder dykes to the overlying volcanic rocks. On that basis, we have identified this unit as the lowest member of the Fairbridge Volcanics: it may correlate with the mainly coarser grained volcaniclastic sediments below the Waringah Limestone Member farther north in the belt.

Unit 2 is represented by coarse volcaniclastic sandstones and conglomerates dominated by basaltic clasts with prominent clinopyroxene phenocrysts. It overlies Unit 1 with a gradational contact, youngs west and is 500–1000 m thick. It also contains numerous dykes compositionally similar to those described from Unit 1.

Unit 3, $\sim$300 m thick, is a regionally extensive (along strike), readily recognisable unit dominated by pillow basalt and monomict breccia with large (up to 2 mm)

Downloaded by [Auckland University of Technology] at 15:24 09 March 2015

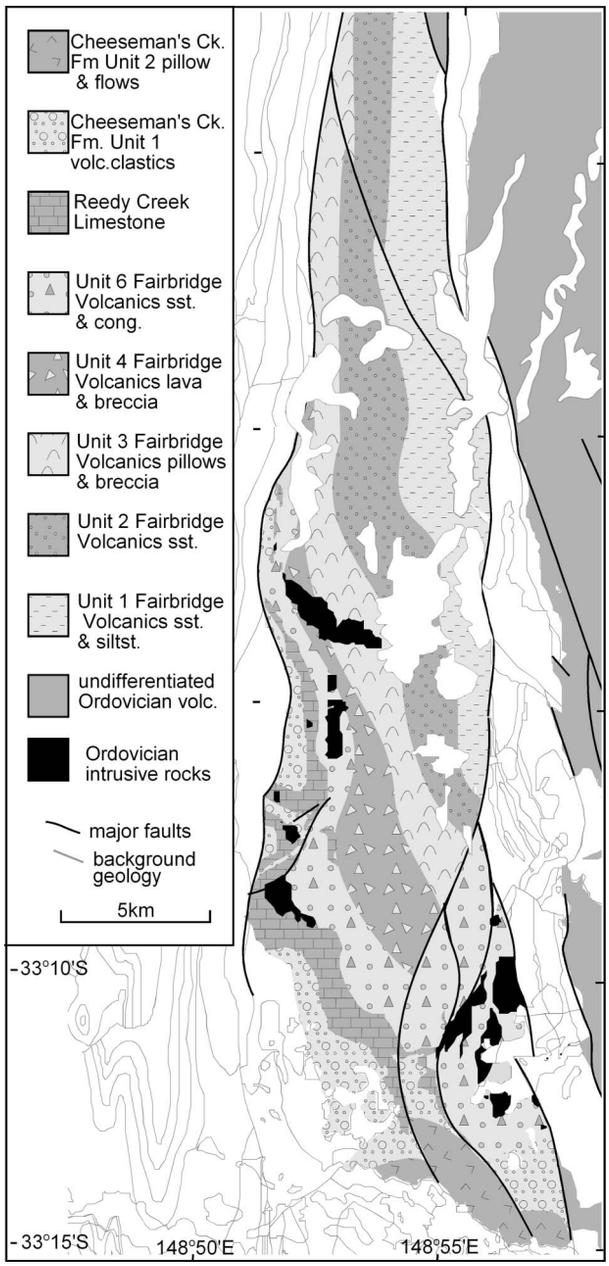

Figure 9 Geological map of the Molong Volcanic Belt north of Orange, towards Molong, showing lithostratigraphic units identified in the Fairbridge Volcanics and Cheesemans Creek formation. See text for details.

clinopyroxene phenocrysts and small plagioclase phenocrysts (<0.8 mm).

Unit 4 consists mostly of andesitic lava breccias and coarse andesitic conglomerates containing abundant plagioclase phenocrysts.

Unit 5 is the small body of Yuranigh Limestone Member that can be correlated approximately in time and facies with the upper Waringah Limestone member (Percival & Glen 2007).

Unit 6 consists of volcaniclastic sandstones and conglomerates, often intensely altered and intruded by Phase 3 felsic igneous rocks and hornblende-bearing dykes. Most clasts in this unit are petrographically and geochemically similar to Unit 4 lavas, but felsic hornblende-bearing clasts similar petrographically to the Copper Hill Suite intrusives (Crawford *et al.* 2007) also occur. In the Yuranigh's Grave area south of Molong, many basalts just above the Yuranigh Limestone Member have abundant, large plagioclase phenocrysts, and are petrographically and geochemically (upper Fairbridge Volcanics: Table 1) similar to Phase 4 shoshonitic basalts in the overlying Cheesemans Creek Formation.

Although more detailed field and geochemical studies are required to thoroughly characterise the Fairbridge Volcanics, several important points emerge from available geochemical data. First, lavas with Zr/Nb values between 24 and 36 (Figure 8c) and P_2O_5 and REE contents matching those of the Walli Volcanics at similar MgO contents (Figure 8c, d) are present mainly in the lower section of the Fairbridge Volcanics (up to and including the lower pillows in Unit 3). Lavas higher in the same sequence, including some of the upper pillow basalts in Unit 3, mainly show significantly lower Zr/Nb values, range to higher P_2O_5 contents and have shoshonitic affinities (Figure 8c, d).

In summary, the Fairbridge Volcanics lavas from the Molong region show a well-defined petrographic and compositional change from basal volcaniclastic rocks with andesitic and basaltic detritus and rare lavas with medium- to high-K calc-alkaline affinities, through pillowed high-K calc-alkaline to shoshonitic basalts and basaltic andesites. An Eastonian hiatus in volcanism, reflected by deposition of the Reedy Creek Limestone before the Phase 4 Cheesemans Creek Formation was deposited, is associated with Phase 3 intrusion of the Copper Hill tonalite–dacite suite of medium-K calc-alkaline felsic magmas. When volcanism resumed (Phase 4), it was more evolved (andesitic) and markedly shoshonitic in character, producing the Cheesemans Creek Formation (see below).

The Oakdale Formation extends along the length of the eastern side of the northern Molong Volcanic Belt. It was previously taken to include most of the Ordovician volcano-sedimentary sequence in the Wellington area (Pogson & Watkins 1998), although we prefer to include it in the Fairbridge Volcanics. In outcrops along the Bell River and along the Mitchell Highway between Molong and Orange (Boulton 2001), the Oakdale Formation is represented by generally monotonous volcaniclastic turbidites with a fine-grained sandstone base fining upwards to volcaniclastic siltstone. Sparse conglomerates carry basaltic and andesitic volcanic clasts.

A number of small felsic quartz + hornblende + plagioclase-phyric fine-grained rocks intrude the Oakdale Formation turbidites and are petrographically similar to the distinctive Phase 3 Copper Hill and Cargo felsic intrusive dacite complexes.

A small, probably fault-bounded area along the Mitchell Highway and Molong Creek previously mapped as Oakdale Formation (Meakin & Morgan 1999) contains basaltic flows, pillows and dolerite intrusions interbedded with minor siltstone and sandstone. Unlike typical Fairbridge Volcanics, these volcanics are aphyric

Downloaded by [Auckland University of Technology] at 15:24 09 March 2015

with abundant small needles of ilmenite and pinkish relatively high-Ti clinopyroxene. Lavas and dolerites both have TiO_2 contents (1.6–2.2%: Table 1) well above any Ordovician lavas recorded from the Molong Volcanic Belt. Sandstones contain detrital quartz (up to 20%) and minor zircons. These rocks are unlike the Oakdale Formation or any other Ordovician unit known in Molong Volcanic Belt and may be better correlated with the nearby Early Devonian Cuga Burga Volcanics (Meakin & Morgan 1999).

CHEESEMANS CREEK FORMATION

The Cheesemans Creek Formation crops out south and west of Molong where it overlies the Reedy Creek Limestone and uppermost Fairbridge Volcanics. Graptolite faunas indicate an early Bolindian age (Pogson & Watkins 1998; Scott *et al.* 1998; Percival & Glen 2007). Our mapping in the Cheesemans Creek and Boree Creek areas shows that this formation can be subdivided into two units (Figure 9).

Unit 1 consists of volcaniclastic sandstones and siltstones, and rare conglomerates extensively intruded by two types of sills. Synsedimentary basaltic andesite sills with peperitic contacts and small plagioclase phenocrysts are the most common, and are intruded by basaltic and andesitic sills with distinctive large plagioclase phenocrysts, similar to those of the overlying Unit 2. Clasts in conglomerates are petrographically similar to Unit 4 of the underlying Fairbridge Volcanics but also include limestones and hornblende + quartz-bearing felsic intrusive rocks similar to the Copper Hill intrusions. Some clasts were hydrothermally altered prior to deposition (pyrite–albite–magnetite–chlorite alteration).

Unit 2 consists almost entirely of distinctive 'big plagioclase' andesite flows and pillows, with plagioclase phenocrysts up to 15 mm long. These lavas are identical petrographically and geochemically (Table 1) to the packages of pillow lavas in siltstones in the Malachis Hill Formation at Bowan Park in the northern Cargo block (Simpson *et al.* 2007), with which they are correlated. Both suites show shoshonitic affinities (Figure 8a, b).

Forest Reefs–Orange–Blayney area

Pogson and Watkins (1998) and Squire and Crawford (2007) showed that the earliest exposed Macquarie Arc rocks in the Cadia–Neville area are feldspathic turbidites of the Weemalla and Coombing Formations (Figure 2). These pass up into pillowed high-K to shoshonitic basalts of the Mt Pleasant Basalt Member just above the base of the Forest Reefs Volcanics, which are in turn overlain conformably by black shales with Gisbornian (Gi2) graptolites. Volcanic lithic breccias increase in abundance up-section and are followed by a polymictic conglomerate and the poorly dated Upper Ordovician Cowriga Limestone Member; a separate unnamed limestone at Sheahan-Grants Mine and dated as Late Eastonian (Packham *et al.* 1999) is correlated with the top of the Bowan Park Limestone Subgroup (Figure 2). Complex volcanic facies of the Forest Reefs Volcanics above this limestone interval represent Phase 4 magmatism and include abundant lava breccias and polymictic conglomerates, volcanic sandstones, and an upper facies dominated by shoshonitic trachyandesitic and trachytic lavas referred to as the Nullawonga Latite Member (Wyborn & Henderson 1996; Squire & Crawford 2007). A high-level hornblende dacite body petrographically and geochemically identical to the Phase 3 Copper Hill Suite dacites intrudes the Cowriga Limestone Member near Browns Creek.

The Forest Reefs Volcanics are the dominant Phase 4 magmatic unit represented in the Cadia–Forest Reefs–Neville region. They are a shoshonitic suite cut by numerous small monzonitic and monzodioritic intrusives, and their petrology and geochemistry are discussed in detail by Blevin (2002), Holliday *et al.* (2002), and Squire and Crawford (2007).

Blayney Volcanics

Squire and Crawford (2007) and Squire and McPhie (2007) provide a comprehensive account of the geology of the Cadia–Neville area in the south-central Molong Volcanic Belt. Here, we focus on the geology and geochemistry of the Ordovician volcanics and associated rocks farther east, in the adjacent Orange–Blayney area. Originally mapped as extensive areas of Blayney Volcanics (Wyborn & Henderson 1996), we have informally subdivided the Blayney Volcanics into two lithostratigraphic units, the lower Blayney Volcanics and upper Blayney Volcanics, and these are overlain by the Phase 4 Millthorpe Volcanics (new unit, defined in Appendix 2). The Blayney Volcanics overlie feldspathic turbidites of the Coombing Formation. Their age is not well constrained, although stratigraphic considerations suggest they may extend down into the top of the Darriwilian (Percival & Glen 2007). SHRIMP U–Pb dating using the AS3 standard zircons of 19 detrital zircon grains in the Coombing Formation shows a single population of Darriwilian age, around 466 ± 4 Ma (Figure 10) (Meffre et al. 2007 figure 9). These zircons are probably derived from intrusive Phase 2 monzodioritic suite rocks such as those of identical age that are conspicuous elements of the Narromine and Cowal Igneous Complexes in the Junee–Narromine Volcanic Belt.

The oldest volcanics in the region are the clinopyroxene + olivine-phyric lower Blayney Volcanics. These are dominantly basaltic lavas and coarse lava breccias with 7–12% MgO, with rare andesites, and no dacites or more evolved lavas (Table 1). Passing up-section, there is a transition into the upper Blayney Volcanics via a gradual increase in the modal abundance of phenocrystic plagioclase. The upper Blayney Volcanics are not comagmatic with the lower Blayney Volcanics, having at any MgO level notably lower Al_2O_3 and higher K_2O and P_2O_5 contents (Figures 8b, c, 11), yet lower Zr, Y and Nb contents, and distinctly high Ti/Zr values (mainly 30–50). Abundant dykes in the underlying Coombing Formation west of the main outcrop area of lower Blayney Volcanics, referred to as the Eaglehawk Basalts by Wyborn and Henderson (1996), match precisely the compositional range of the upper Blayney Volcanics, and are clearly feeders to this unit (Squire & Crawford 2007). REE patterns for the upper Blayney Basalts and

Downloaded by [Auckland University of Technology] at 15:24 09 March 2015

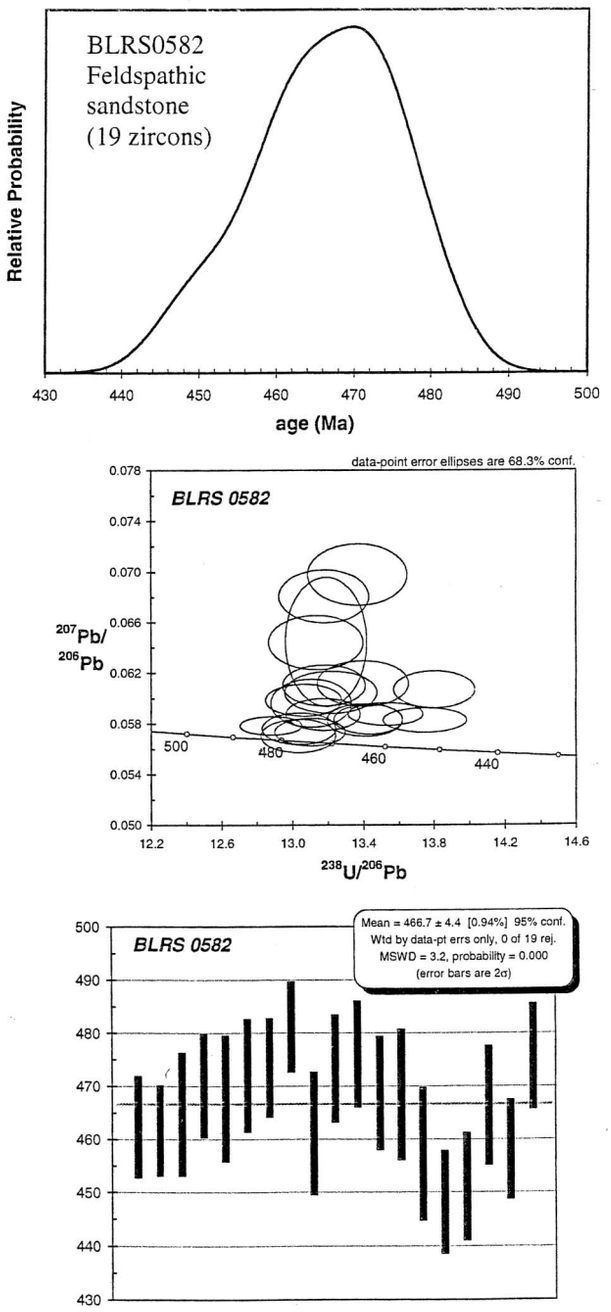

Figure 10 (a) Near-symmetrical bell-shaped probability plot of SHRIMP U–Pb ages on detrital zircons from Coombing Formation feldspathic sandstone BLRS0582 showing only Ordovician ages, and one likely provenance. (b) Tera–Wasserburg concordia plot of total $^{207}Pb/^{206}Pb$ *vs* total calibrated $^{238}U/^{206}Pb$ for same zircon population. (c) Weighted average plots showing calculated age ranges for the 19 analysed zircons.

correlated dykes show slight LREE enrichment (Figure 12a). The upward transition from relatively primitive plagioclase-phenocryst-free lower Blayney Volcanics to the commonly plagioclase-phyric upper Blayney Volcanics matches the same petrographic transition evident from Unit 2 to Unit 4 in the Fairbridge Volcanics in the northern Molong Volcanic Belt.

Byng Volcanics

The Late Ordovician Byng Volcanics, dominated by mafic lavas, cumulates and volcaniclastics (Pogson & Watkins 1998), outcrop east of Orange as north-northwest-trending fault-bounded slices with their distribution controlled by a set of regional north-northwest-trending, east-dipping structures related to the dominant regional fault array, in particular to the major east-dipping Godolphin Fault system. The latter forms a composite portion of a duplex/imbricate thrust system marking part of the western boundary of the deformed Hill End Trough (Glen & Watkins 1999).

Ambiguity has arisen as to the distribution of the Byng Volcanics, since its identification was largely based on a characteristic strong aeromagnetic response that contrasts with the featureless Blayney Volcanics. However, our work has shown that volcanics mapped as Byng Volcanics north and west of Blayney (Pogson & Watkins 1998) are very different petrographically and geochemically from the Byng Volcanics east and north-east of Blayney. In summary, the former have been removed from the Byng Volcanics and assigned to a new stratigraphic unit, the Millthorpe Volcanics, that has strong facies, petrographic and geochemical similarities to the Forest Reefs Volcanics west of the Carcoar Fault. The name Byng Volcanics is kept for those mainly basaltic rocks occurring as fault-bounded sequences east of Orange, which are often associated with comagmatic ultramafic cumulates ('limburgite suite' of Barron & Barron 1996).

The Byng Volcanics are dominantly primitive basalts, extending via increasing amounts of accumulated olivine phenocrysts, to ultramafic lava compositions (Figure 11). Olivine-rich cumulates ranging from wehrlites through clinopyroxene–dunites to dunites (Barron & Barron 1996) are commonly associated with the Byng Volcanics and probably represent either basal crystal-rich portions of thick, fluid flows, or small localised magma chambers associated with Byng magmatism. With decreasing MgO, basalts contain less olivine and more clinopyroxene phenocrysts, and the most evolved Byng Volcanics reach basaltic andesite compositions and also contain uncommon plagioclase phenocrysts (Williams 1999).

The Byng Volcanics define a broad but coherent compositional field on element–MgO diagrams (Figure 11), extending from basaltic andesite to ultramafic compositions. A major conclusion of this study is that at least part of the Byng Volcanics is comagmatic, and thus broadly contemporaneous, with the shoshonitic upper Blayney Volcanics, a conclusion strongly supported by variation diagrams in Figure 11, REE patterns (Figure 12a) and Nd isotopic compositions (Table 2). The shoshonitic affinities of the Byng lavas, including the ultramafic lavas, have been demonstrated via a melt inclusion study of fresh clinopyroxene phenocrysts (Williams 1999), further supporting the link between the Byng and upper Blayney Volcanics.

Millthorpe Volcanics

Our mapping, and especially that by Duerden (1999), has demonstrated clearly that rocks mapped previously as

Downloaded by [Auckland University of Technology] at 15:24 09 March 2015

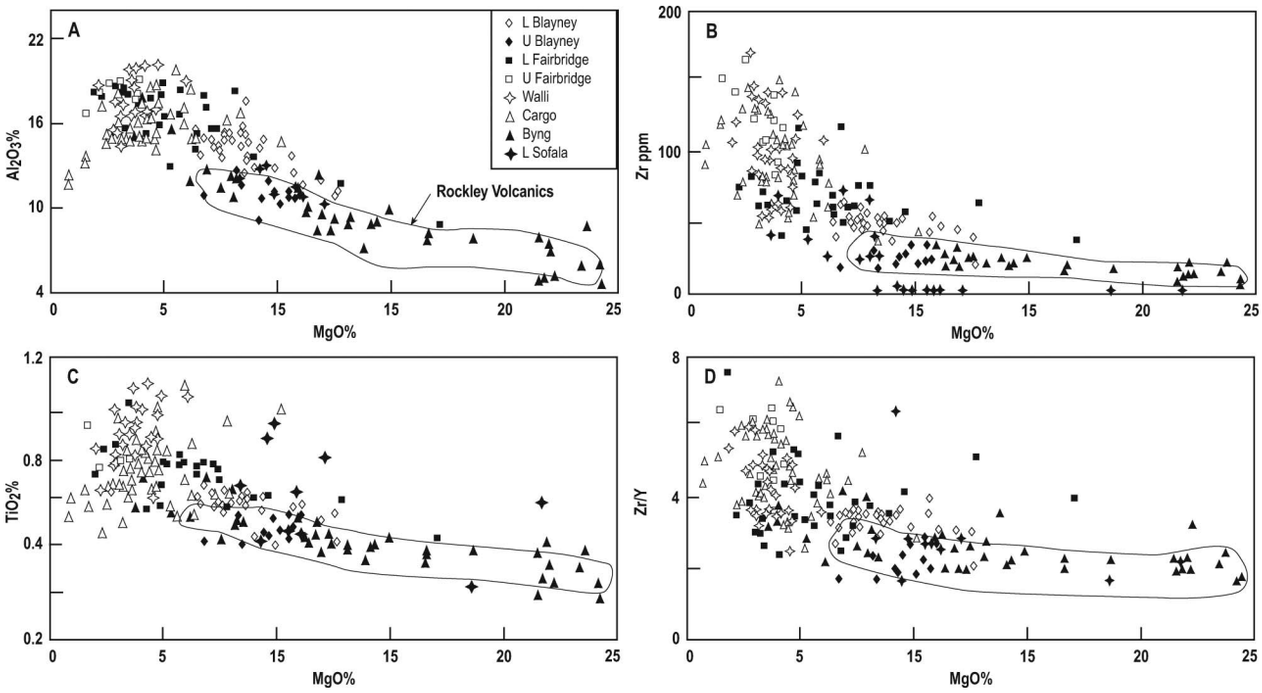

Figure 11 Variation diagrams of (a) Al_2O_3, (b) Zr, (c) TiO_2 and (d) Zr/Y *vs* MgO for Phase 2 lavas from the Molong and Rockley–Gulgong Volcanic Belts, showing the striking similarity of Byng and Rockley Volcanics, and likely correlation of upper Blayney Volcanics with the Byng Volcanics. Most data for the Rockley Volcanics from Pogson and Watkins (1998).

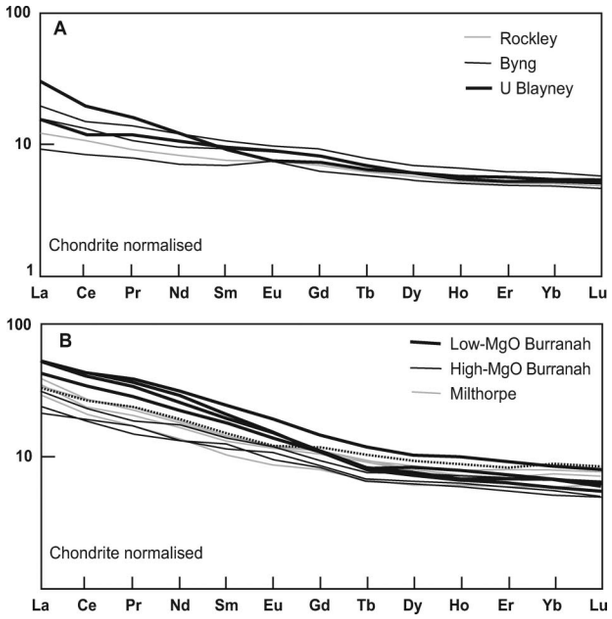

Figure 12 Chondrite-normalised REE patterns of (a) Phase 2 lavas in the Molong (Byng and upper Blayney Volcanics) and Rockley–Gulgong (Rockley Volcanics) Volcanic Belts and (b) Phase 4 Millthorpe Volcanics (Molong Volcanic Belt) and Burranah Volcanics (Rockley–Gulgong Volcanic Belt).

Byng Volcanics west and north of Blayney (Pogson & Watkins 1998) are dominantly volcaniclastic rocks, with common basaltic to basaltic andesite lavas, all petrographically and compositionally unlike the main Byng Volcanics. Just west of Browns Creek mine, there is a passage upward from typical upper Blayney Volcanics into more evolved, plagioclase-phyric lavas we assign to the Millthorpe Volcanics (Appendix 2). Similarly, rocks now mapped as Millthorpe Volcanics occur above the poorly dated Upper Ordovician Cowriga Limestone Member at several locations, although the nature of the contacts is unclear. We suggest that the Millthorpe Volcanics represent Phase 4 magmatism and are correlated with the upper part of the Forest Reefs Volcanics (Squire & Crawford 2007) that occur on the western side of the Carcoar Fault. The upward passage from basalt-dominated upper Blayney Volcanics to the generally more evolved Millthorpe Volcanics matches that in the Molong region, where the upper Fairbridge Volcanics pass, via limestones, up into the andesite-dominated Cheesemans Creek Formation.

As shown on Figure 8a, b, the Millthorpe Volcanics are dominated by evolved basaltic and basaltic andesite compositions with high P_2O_5 and K_2O typical of shoshonitic suites and $Zr/Nb = 7-15$ and somewhat LREE-enriched patterns (Figure 12b). A greater volume of evolved lavas occurs in the Forest Reefs Volcanics than in the Millthorpe Volcanics.

Several significant monzodioritic to monzonitic intrusions occur in this area, notably the Moorilda Monzonite. On the basis of intrusive relationships and correlation with similar bodies in the southern Molong Volcanic Belt, these rocks are believed to have been emplaced at *ca* 440 Ma. Their geochemistry and geochronology are discussed in Squire and Crawford (2007).

Downloaded by [Auckland University of Technology] at 15:24 09 March 2015

Downloaded by [Auckland University of Technology] at 15:24 09 March 2015

Bodangora area

Reconnaissance mapping and sampling of the block of Ordovician volcanics north of Wellington, at the northern exposed tip of the Molong Volcanic Belt, show a west-dipping succession of volcanic and volcaniclastic rocks that show the same up-to-the-west increase in K_2O and P_2O_5, and increasing SiO_2 as noted farther south at Molong and Blayney. Primitive clinopyroxene + olivine-phyric basalts compositionally akin to the Fairbridge Volcanics occur on the eastern side of the block, and lavas become more evolved and more shoshonitic up-section to the west.

The occurrence of shoshonitic lavas with characteristic apatite microphenocrysts around the Kaiser prospect in the very eastern extent of the Bodangora area may suggest significant fault-related repetition of the western shoshonitic sequence.

ROCKLEY–GULGONG VOLCANIC BELT

Unlike the Molong Volcanic Belt, in which Ordovician volcanic and volcaniclastic rocks extend continuously along strike for ~150 km, Ordovician volcanic rocks constituting the Rockley–Gulgong Volcanic Belt occur as isolated, discrete, largely fault-bounded blocks. From south to north, these include the Triangle and Rockley Volcanics in the Rockley area, the Sofala Volcanics in the Sofala area, the Coomber Formation east of Mudgee and in the Lue area, the Burranah Formation between Mudgee and Gulgong, and the Tucklan Formation south of Dunedoo. Percival (1999) and Percival and Glen (2007) reviewed available biostratigraphic age constraints on these units in the northern part of the belt. Carr *et al.* (2003) reported geochemical data for rocks from the latter three areas.

The Rockley Volcanics remain relatively poorly known, but our sampling, coupled with other studies (Pogson & Watkins 1998; Meakin & Morgan 1999; Murray & Stewart 2000; Carr *et al.* 2003; Meffre *et al.* 2007), indicates that this unit consists principally of volcaniclastic rocks. Biostratigraphic work around Oberon (Murray & Stewart 2000) demonstrated the presence of Lower Ordovician chert (Budhang Chert) overlain by fine-grained volcaniclastic siltstone and sandstone. These cherts, which Percival and Glen (2007) suggested to be part of the Adaminaby Group, are separated by a fault (Meffre *et al.* 2007) from Middle Ordovician sandstone, siltstone, chert and minor conglomerate with coarse clinopyroxene-phyric basalt clasts. Farther west, near Rockley and at Dog Rocks, ultramafic rocks of the Rockley Volcanics include common exceptionally olivine-rich picritic lavas and clinopyroxene + olivine-phyric basalts and breccias that are identical petrographically and geochemically (Table 1; Figures 11, 12a) to the Phase 2 Byng Volcanics of the Molong Volcanic Belt. This striking similarity between these two distinctive units provides a confident tie between the Molong and Rockley–Gulgong Volcanic Belts.

Reconnaissance mapping in the Sofala area (Meffre *et al.* 2007) has shown that the Sofala Volcanics consist of a thick fining-upwards sequence of Middle (late Darriwilian) to Late Ordovician (mid-late Bolindian) chert, sandstone and conglomerate with subordinate clinopyroxene-phyric basalts. At Palmers Oakey, they consist of coarse-grained, polymict conglomerate dominated by clasts of clinopyroxene-phyric basalt and rare Eastonian limestone blocks. These conglomerates are interbedded with clinopyroxene-rich sandstone, siltstone and black chert. The Sofala Volcanics near Sofala consist of a thick sequence of monomict and polymict conglomerates with clasts of clinopyroxene-phyric basalts interbedded with volcaniclastic sandstone and siltstone. These volcaniclastic rocks are truncated by southwest-dipping fault zones containing tightly folded black chert (Meffre *et al.* 2007). Towards the south (and at the top of the sequence), the conglomerate is affected by pervasive carbonate alteration which hosts numerous small, historical gold mines and also contains limestone blocks dated as Eastonian (Percival *et al.* 1999; Percival & Glen 2007). The zone of carbonate alteration is overlain by volcaniclastic sandstone containing crinoid stems and brachiopods. Minor conglomerates with plagioclase-phyric and aphyric clasts also occur in this unit.

All Sofala Volcanics analysed (this study; Watkins 1998; Carr *et al.* 2003) are trachybasaltic to trachyandesitic compositions with medium to low TiO_2 and generally high K_2O and P_2O_5 (Table 1). The lower Sofala Volcanics show relatively primitive shoshonitic compositions, very similar to the upper Blayney and Byng Volcanics basalts (Figure 11).

Most rocks of the Coomber Formation east of Mudgee and west of Capertee have a strong cleavage and are predominantly fine-grained volcaniclastic sandstone and siltstone, with minor chert outcropping along the eastern boundary of the block. Clinopyroxene-phyric basalt and biotite monzonite intrusions were noted in a small fault block 15 km southeast of Mudgee along the Cudgegong road. A thick sequence of cleaved Ordovician volcaniclastic sandstone and siltstone, with minor sparsely plagioclase-phyric broadly andesitic lavas, crops out along the road between Turon Gates and Capertee.

The Burranah Formation crops out in a fault-bounded north-trending belt of rocks about 20 km long and 5 km wide north of Mudgee. It is dominated by a sequence of mafic to intermediate volcaniclastic sandstone and breccia with minor coherent lava, and is estimated to have a total thickness of 2.5 km (Watkins 1996). The volcanic rocks are intruded by a number of small bodies (up to 3 km long and 700 m wide, but usually much smaller) of mainly medium- to coarse-grained monzodiorite, considered to be broadly comagmatic with the host volcanics (Watkins 1996). Resedimented syn-eruptive deposits occur throughout the Burranah Formation as coarse, thickly bedded and unsorted monomictic volcanic breccias with blocks up to 20 cm across in a sandy matrix. Less common coherent lavas occur as massive units up to 5 m thick, rarely pillowed, with varying proportions of augite and plagioclase phenocrysts.

Interbedded with the volcanic facies in the Burranah Formation, and more abundant in the upper part of the block, are massive black (often pyritic) mudstones,

graded turbiditic sandstones, and minor conglomerate and breccia units that contain clasts of limestone and oxidised red lavas. Corals and conodonts in the limestone clasts in mass-flow units in the Burranah Formation indicate a mid-Eastonian age (Percival 1999; Percival & Glen 2007). This suggests that the Burranah Formation volcanics may correlate with the Millthorpe Volcanics, Forest Reefs Volcanics and Cheesemans Creek Formation.

Watkins (1996, 1999) and Carr *et al.* (2003) provided geochemical data for 30 lavas from the Burranah Formation. Four of these are quite primitive clinopyroxene + olivine-phyric basalts (8.8–13.2% MgO) with the very low Zr abundances (26–52 ppm) that characterise the upper Blayney Volcanics in the Blayney area to the southwest in the Molong Volcanic Belt (Table 1). REE patterns (Figure 12b) of the more mafic Burranah lavas match those for the basaltic rocks from the upper Blayney and Millthorpe Volcanics, and the more evolved lavas in the Byng Volcanics on the southeastern margin of the Molong Volcanic Belt. Age-corrected (450 Ma) ε_{Nd} values for three Burranah trachyandesites range from +5.55 to +6.16 (Table 2) (Watkins 1996, 1999), suggesting that this unit may contain both late Phase 2 and Phase 4 magmatic suites.

KIANDRA VOLCANIC BELT

We conducted a reconnaissance mapping, sampling and analytical program of Ordovician rocks in the Kiandra–Snowy Mountains region. Wyborn *et al.* (1990) described and mapped a conformable contact between the Adaminaby Group and the Nine Mile Volcanics from Jagungal to the Eucumbene River in the Snowy Mountains. Detailed remapping of this area (Meffre *et al.* 2007) has shown that this contact is faulted. The major volcanic unit studied, the Nine Mile Volcanics, shows clear shoshonitic affinities (Owen & Wyborn 1979). Age constraints on these rocks are restricted to Gisbornian graptolites and conodonts (Percival & Glen 2007).

SIGNIFICANCE OF PHASE 3 MAGMATISM—COPPER HILL SUITE

Rocks belonging to the Phase 3 magmatic event occur in each of the three major volcanic belts of the disrupted Macquarie Arc. At most localities, they typically occur as small high-level intrusive bodies rarely larger than 500 m across, with the distinctive phenocryst assemblage plagioclase–quartz–hornblende–Ti-magnetite; a characteristic occurrence as a small intrusion several hundred metres across is on Jenkins Road, west of Mudgee in the Rockley–Gulgong Volcanic Belt. However, several larger plutons have been defined by drilling in the Cowal Igneous Complex. As the Copper Hill Complex in the Molong area is perhaps the best known of these occurrences (Blevin 2002), this widespread magmatic suite is referred to as the Copper Hill Suite. In the Cowal Igneous Complex and some of the intrusive sheets in the Narromine Igneous Complex, representative bodies are more holocrystalline textured, although they show the same mineralogy as porphyritic variants.

Copper Hill Suite rocks from the Narromine Igneous Complex and from Copper Hill have been radiometrically dated. Perkins *et al.* (1995), using $^{40}Ar/^{39}Ar$ dating on hornblendes, produced an age of 449.1 ± 1 Ma for a Copper Hill diorite, and using SHRIMP U–Pb zircon dating obtained an age of 450 ± 6 Ma for a Copper Hill dacite porphyry.

We have SHRIMP-dated zircons from two Copper Hill Suite samples from the Narromine Complex, a dacite from drillhole NACD83 and a granodiorite from NACD 86 (Crawford *et al.* 2007). All zircons studied in both rocks have well-developed euhedral outer zones that record ages of 441 ± 5 Ma in the dacite, and 449 ± 5 Ma in the granodiorite, averaging at 445 Ma (mid-Bolindian). These match dates obtained from the Copper Hill rocks. A 453 ± 5 Ma LA-ICPMS date on zircons in a volcaniclastic sandstone rich in detritus and lithic clasts of Copper Hill-type dacite porphyries in the Ranch Member of the Bowan Park Limestone Subgroup at the northern end of the Cowal block (Simpson *et al.* 2007; Meffre *et al.* 2007) suggests that Phase 3 magmatism may have commenced before 450 Ma.

The geochemistry of the Copper Hill Suite Phase 3 magmatism is discussed in more detail in Crawford *et al.* (2007). As demonstrated by Blevin (2002) for the Copper Hill Complex, the Copper Hill Suite is a medium-K calc-alkaline suite notably less enriched in LILE than either the Phase 2 high-K and shoshonitic rocks, or the Phase 4 shoshonites. The dominant magma type is dacitic in composition, and more mafic varieties (particularly in the Cowal block) are cumulates relatively enriched in hornblende, Ti-magnetite and calcic plagioclase. The Copper Hill Suite magmas were probably derived through partial melting of low-K metabasic rocks in the lower crust Crawford *et al.* (2007). Although it is possible that they were produced by extended fractionation from typical medium-K calc-alkaline basalts, the absence of appropriate parental magmas of Phase 3 age (see below) makes this unlikely.

In summary, the Phase 3 medium-K calc-alkaline magmas represent a magmatic pulse that records a striking departure from the Phase 2 trend towards shoshonitic magmas. Concomitant with Phase 3 magmatism is widespread uplift, erosion and limestone deposition. The tectonic significance of this is discussed below.

FIFIELD COMPLEXES

A series of semi-vertical pipe-like intrusive complexes known as the Fifield complexes lies west of the Junee–Narromine Volcanic Belt and intrude deformed Ordovician metasediments of the Girilambone Group. The Fifield complexes occur in a north-trending belt 80 km wide and 540 km long and have been identified as Alaskan-type ultramafic–mafic complexes that host minor PGE mineralisation (Barron 1988; Barron *et al.* 1991; Elliott & Martin 1991a, b). At least 40 intrusions have been identified, either from poorly exposed outcrop or from their strong aeromagnetic signatures. For

Downloaded by [Auckland University of Technology] at 15:24 09 March 2015

Downloaded by [Auckland University of Technology] at 15:24 09 March 2015

details of the geology and geological settings of these intrusions see Barron (1988), Elliott and Martin (1991a, b) and Sherwin (1996).

The intrusions are all zoned and can be broadly divided into ultramafic and felsic zones. The ultramafic series rocks generally consist of dunites, peridotites, wehrlites, clinopyroxenites, biotite–magnetite pyroxenites, hornblende pyroxenites and hornblendites. The felsic series rocks are generally monzonites, monzodiorites and diorites (Agnew 1987; Stojanovic 1995; Barron 2001). Magnetite is an abundant accessory phase, accounting for the very strong magnetic signatures of the intrusions (Spencer 1990). Barron *et al.* (1991) used the Al-in-hornblende geobarometer to show that hornblendes in the major complexes crystallised at pressures between 400 and 800 MPa, not *in situ*, since the metasedimentary host rocks show only biotite- to actinolite-grade greenschist metamorphic assemblages.

There is a general consensus among previous workers that parental magmas to the felsic (or feldspathic) series of the intrusive complexes were high-K, LREE-enriched shoshonitic magmas, identical to shoshonitic magmas of Late Ordovician and earliest Silurian age elsewhere in the Junee–Narromine and Molong Volcanic Belts (Agnew 1987; Barron 1988; Wyborn 1992; Stojanovic 1995; Andrew *et al.* 1995; Sproule *et al.* 1996; Glen *et al.* 1998; Falloon 2001). However, no such consensus has been reached regarding the parental magmas to the ultramafic series of these complexes, with both Xue (1990) and Barron *et al.* (1991) arguing that the ultramafic series are unrelated to the felsic series rocks, and that the parental magma of the ultramafic cumulates was tholeiitic. Most ultramafic series rocks are cumulates, and their whole-rock compositions do not represent any liquid composition. Recent geochemical work (Sproule *et al.* 1996; Falloon 2001) suggested that the ultramafic series rocks were also produced from a shoshonite parent magma (albeit at the mafic end of the shoshonitic series) and that the felsic series is indeed comagmatic with the mafic–ultramafic rocks. This conclusion was based on: (i) the obvious intimate intrusive relationship to the felsic series rocks; and (ii) the overall calc-alkaline and potassic character of the ultramafic series rocks including (a) the abundance of olivine and clinopyroxene and relatively late appearance of plagioclase, (b) the abundance of early crystallising magnetite suggesting high f_{O2}, (c) the presence of significant hornblende, suggesting high f_{H2O} and (d) the presence of accessory biotite, and hornblende with significant K_2O content (the average in Owendale pyroxenite hornblendes is $0.87 \pm 1.10\%$: Barron 1988).

Our new whole-rock and mineral chemical data (including data in Falloon 2001) indicate that any involvement of a tholeiitic melt in the generation of these complexes is unlikely, and that they crystallised from shoshonitic magmas that may have initially had very primitive compositions, similar to those in the Byng and Rockley Volcanics. Falloon (2001) demonstrated that the average and representative clinopyroxene compositions from pyroxenites of the Owendale complex are identical to clinopyroxene compositions in the shoshonitic Byng Volcanics. Similarly, he showed that spinels from dunites of the Owendale complex are identical to spinels in ultramafic cumulates associated with the Byng Volcanics and in olivine phenocrysts in mafic Byng Volcanics.

Very olivine-phenocryst-rich ultramafic lavas in the Byng Volcanics are identical to rocks of the Owendale complex in terms of key major-element compositions, and similar relationships are evident from all other key major and trace elements (Falloon 2001). Although Owendale complex rocks have REE patterns indicating a shoshonitic parentage, Falloon (2001) showed that the parental magmas of this complex may have had even higher REE abundances and stronger LREE-enrichment than the parental Byng Volcanics.

The immobile incompatible element geochemistry of some Owendale complex ultramafic rocks is presented as a normalised multi-element plot in Figure 13a. Although the dunites and peridotites of the Owendale complex are adcumulates, their incompatible element contents will generally be representative of a magma because the dunites and peridotites are dominated by olivine, which contains effectively zero incompatible elements. Consequently, it only requires a very small percentage of trapped intercumulus melt to dominate the incompatible element signature of the cumulate. The general similarity of the Byng ultramafic lava pattern to the Owendale cumulate patterns supports their crystallisation from similar shoshonitic magmas. Figure 13b shows that there is also an exact match in

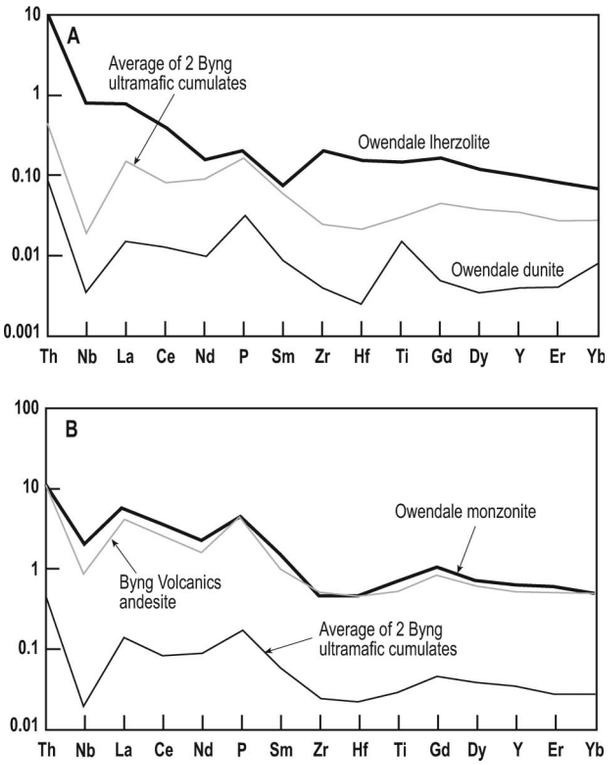

Figure 13 N-MORB normalised multi-element plots (normalising values from Sun & McDonough 1989) of (a) Owendale complex ultramafics compared with average of two olivine-accumulative Byng Volcanics ultramafic lavas, and (b) a Byng Volcanics andesitic lava compared with a monzonite from the Owendale complex, and average of two olivine-accumulative Byng Volcanics ultramafic lavas.

Downloaded by [Auckland University of Technology] at 15:24 09 March 2015

patterns between the monzonite analysed from the Owendale complex and the most evolved Byng lava in our data set, and that the patterns for the analysed ultramafic series rocks from the Owendale complex, despite scatter, clearly show the same general features as the Byng shoshonite lavas and associated cumulates.

Stojanovic (1995) reported initial ε_{Nd} values of +4.9 and 5 for two monzonites from the Tout complex. Sproule *et al.* (1996) reported initial ε_{Nd} values of −0.91 and +3.3 for two Owendale complex cumulates, and argued on the basis of this and Re–Os isotopic data that these low values reflected interaction of a basaltic magma derived from a depleted mantle source with minimal crustal input, with an LREE-enriched fluid phase that had equilibrated with Proterozoic crust. However, coupled with the fact that (i) our REE data indicate that the Owendale parental magmas probably had stronger LREE enrichment than the Byng shoshonites, and (ii) the Fifield complexes clearly post-date latest Ordovician or earliest Silurian deformation in the region, we believe that the parental magmas to these complexes were similar to the Early Silurian Nash Hill Volcanics. As noted earlier, the Nash Hill Volcanics are more strongly REE-enriched and have significantly lower ε_{Nd} values (+4 to +2) than any preceding Late Ordovician magmas in the Macquarie Arc. Thus, although more detailed study of the Nash Hill Volcanics and the Fifield complexes is clearly warranted, we are confident that all available data support the derivation of the Fifield complexes from mafic and ultramafic shoshonitic magmas of Early Silurian age, akin to the Nash Hill Volcanics. This magmatism post-dated the Macquarie Arc *sensu stricto*.

SUMMARY AND CONCLUSIONS

Temporal compositional trends and correlations in the Macquarie Arc

No strata or volcanics with ages between late Bendigonian and early Darriwilian (i.e. between *ca* 475 and *ca* 466 Ma) are known from any of the three main volcanic belts of the fragmented Macquarie Arc. This may reflect a true hiatus in sedimentation and magmatism, or removal of strata deposited in this interval by subsequent erosion. Although we cannot preclude the latter possibility, we prefer the interpretation that a 9 million year hiatus affected the Macquarie Arc between the Early Ordovician Phase 1 magmatism, and the Middle Ordovician Phase 2 magmatism. The basis for this preference is that there is evidence for uplift and erosion of the Hensleigh Siltstone in the Wahringa area, south of Wellington in the Molong Volcanic Belt. There, limestone clasts with Bendigonian conodonts identical to those in the Hensleigh Siltstone carbonates occur in a breccia near the base of the Fairbridge Volcanics (Percival & Glen 2007). The breccia, in turn, is overlain by shallow-water limestones not older than Darriwilian, suggesting regional uplift and a hiatus in sedimentation. Similarly, Simpson *et al.* (2005) recorded clasts of Nelungaloo Volcanics in the basal Goonumbla Volcanics.

The Middle to Late Ordovician magmatic history of the Macquarie Arc is considered in terms of three magmatic phases (Figure 2).

Phase 2 includes Middle Ordovician magmatic units emplaced or erupted before the Eastonian regional uplift and limestone deposition episode, and is apparently restricted to the western side of the Molong Volcanic Belt and the Junee–Narromine Volcanic Belt.

Phase 3 is represented by the widespread but relatively small-volume Copper Hill Suite of medium-K calc-alkaline largely felsic rocks that occurs in all three volcanic belts, but is probably best represented by the Copper Hill pluton, and in the Cowal and Narromine Igneous Complexes. These high-level intrusive rocks were emplaced mainly between 456 and 445 Ma, during the Eastonian regional uplift event, and were rapidly exposed and eroded, since the petrographically distinctive plagioclase + hornblende + quartz-phyric detritus occurs in the Eastonian (mid-Ea1) Ranch Member of the Bowan Park Limestone Subgroup in the Cargo block, and also in the Molong area.

Phase 4 magmatism is represented by all the volcanics (mainly shoshonitic lavas) and their intrusive counterparts above the Eastonian limestone interval. These occur in all three major volcanic belts. The trend from Phase 2 submarine basaltic and basaltic andesite lavas through abundant Phase 4 shoshonitic trachyandesites, to late and less voluminous shoshonitic trachytic lavas and their high-level intrusive counterparts is identical to the Late Miocene shoshonitic volcanoes in Fiji (Squire & McPhie 2007), although the latter extend to more unfractionated (10% MgO) compositions than the Goonumbla and Wombin Volcanics in their lower pillowed sections (Rogers & Setterfield 1994).

PHASE 2 MAGMATISM

Phase 2 magmatism shows a progressive change in composition from typical oceanic arc-type lavas represented by the medium- to high-K basalts, andesites and rare dacites of the Cargo block (and correlates in the Parkes Volcanics of the Junee–Narromine Volcanic Belt) and the dominantly basaltic lower Fairbridge Volcanics of the Molong Volcanic Belt, to high-K calc-alkaline basalts and basaltic andesites of the basal Goonumbla Volcanics, lower Blayney Volcanics and Fairbridge Volcanics. These pass up, in turn, to the shoshonitic basalt-dominated volcanics of the Mt Pleasant Basalt Member, upper Blayney Volcanics, and Byng Volcanics. This temporal change in compositions is shown by the plot (Figure 14a) of Zr/Nb *vs* chondrite-normalised La/Sm ratio [i.e. (La/Sm)n]. The most arc-like lavas (Cargo, Walli and lower Fairbridge Volcanics) have the highest Zr/Nb and flattest LREE-slopes [lowest (La/Sm)n], and these change progressively to lower Zr/Nb and steeper LREE patterns in Phase 4 magmas, reaching peak enrichment in the Early Silurian Nash Hill Volcanics. Only some of the Byng Volcanics ultramafic lavas are exceptions to this, having (La/Sm)n values between 1.3 and 2.3.

The shift during the Phase 2 Middle Ordovician magmatism in the Macquarie Arc from medium-K calc-alkaline to high-K and shoshonitic compositions is

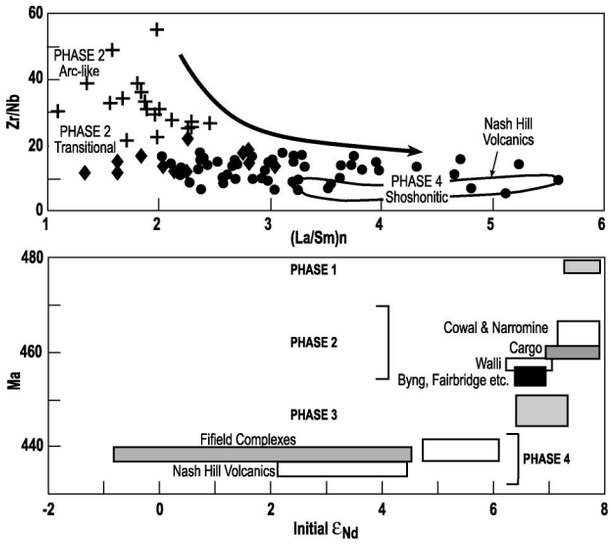

Figure 14 (Top) Zr/Nb versus LREE-enrichment for Phase 2 arc-like lavas (Cargo, Walli, Parkes, basal Fairbridge Volcanics – all + symbols), Phase 2 transitional lavas (Byng, Rockley, Blayney, upper Fairbridge Volcanics, Basal Mafic Unit of Goonumbla Volcanics and Mt Pleasant Basalt Member – all σ symbols), and Phase 4 shoshonitic lavas – all λ symbols. (Bottom) Initial ε_{Nd} versus age for the major magmatic phases that constructed the Macquarie Arc.

accompanied by a shift in ε_{Nd} values from +7 to +8 in the Cargo lavas and Narromine and Cowal Igneous Complex diorites, to +6 to +7 in the more potassic rocks occurring below the hiatus defined by the limestones best developed in the Junee–Narromine and western Molong Volcanic Belts (Figure 14b). A pronounced change to lower ε_{Nd} values is recorded by those shoshonitic lavas and intrusive rocks representing Phase 4 magmatism. Further work is required to determine whether this represents the arrival of a more crustal component (e.g. subducted sediments) in the mantle source or greater amounts of crustal interaction prior to eruption of Phase 4 magmas as they traversed the newly thickened crust.

The strong compositional evidence that the Byng Volcanics, upper Blayney Volcanics and Rockley Volcanics are comagmatic raises several important points. First, it is likely that the Rockley Volcanics were presumably linked to the Byng Volcanics and have perhaps been faulted off the eastern margin of the Molong Volcanic Belt, being displaced eastward toward their present position (see restorations in Glen *et al.* 2007c). Second, the Byng and Rockley Volcanics (and especially the ultramafic members thereof) are limited to the very eastern side of the Molong Volcanic Belt and the Rockley–Gulgong Volcanic Belt, whereas farther west, parental magmas experienced far more fractionation, and no lavas approaching ultramafic compositions are recorded in the Junee–Narromine Volcanic Belt. Even though the high-MgO Byng lavas are ultramafic simply because of olivine accumulation, olivine compositions (Williams 1999) indicate that the magmas from which these formed were extremely primitive and had experienced little fractionation *en route* from their mantle source. This implies easy access to eruption for the lavas along the eastern side of the Molong Volcanic Belt east and south of Orange, suggesting that they were forming and erupting during a time of major extension along the margin of what was probably a rifting arc setting. Such primitive lavas were not passing through the main plumbing systems of an arc volcano (such as the Cargo Volcanics, which always have MgO <6%). Furthermore, the absence of evolved andesites and dacites in the Blayney, Byng and Rockley Volcanics also rules against formation in an arc-type central volcano. This suggests more rapid rifting and collapse of the arc than that which affected Fiji in the Late Miocene and Early Pliocene, where shoshonitic and high-K calc-alkaline volcanoes form at intervals along lineaments parallel to the arc rifts (Squire & Crawford 2007), and contain andesitic and sometimes more felsic lavas.

Such magnesian compositions are relatively rare in intra-oceanic or continental-margin arcs, and are usually associated with arc splitting and fragmentation of the arc-bearing plate (Kamenetsky *et al.* 1995). The key point is that in the Blayney and Byng Volcanics, we are seeing a temporal transition from high-K calc-alkaline magmatism to more unfractionated shoshonitic magmatism, the latter recording an actively extensional setting.

As discussed in Squire and Crawford (2007), a similar change in magma compositions has accompanied the termination of subduction and splitting of the plate bearing the Fijian section of the Late Eocene–Miocene Vitiaz arc. Late Miocene–Early Pliocene arc volcanism in Fiji was mainly medium-K calc-alkaline in nature. Due to Early Pliocene rotation and rifting of the arc (*ca* 5.5–3 Ma), high-K calc-alkaline and shoshonitic volcanoes formed along three broad lineaments (Gill & Whelan 1989) marginal to the main mass of arc crust and parallel to developing spreading centres in the adjacent North Fiji Basin. Volcanic centres are mainly 30–50 km apart. The medium-K calc-alkaline lavas have Zr/Nb values around 40, whereas the high-K and shoshonitic lavas are both more mafic than the medium-K lavas, and have Zr/Nb values mainly between 20 and 25 (Gill & Whelan 1989; Rogers & Setterfield 1994; Verbeeten 1996), matching closely the changes in the Macquarie Arc Middle Ordovician volcanics.

PHASE 3 MAGMATISM

Our radiometric age constraints indicate that the Copper Hill Suite was emplaced between *ca* 456 Ma and 445 ± 4 Ma. At the time when it was interrupted by the Copper Hill Suite magmatic event, Phase 2 magmatism was experiencing a transition from medium-K and high-K calc-alkaline lavas to shoshonitic lavas. The immediately following Phase 4 magmatism was almost entirely shoshonitic, and dominated by more evolved compositions than the shoshonites erupted late in Phase 2 magmatism. Whatever caused this sharp interruption to the transition from Phase 2 shoshonites to early Phase 4 shoshonites, and the brief reversion to medium-K compositions of the Phase 3 Copper Hill Suite, it was a relatively brief, transient event.

Phase 3 magmatism is intimately associated with the Eastonian limestone hiatus and, in the west, significant regional uplift and erosion (Glen *et al.* 1998; Packham

Downloaded by [Auckland University of Technology] at 15:24 09 March 2015

et al. 2003). Coupled with the fact that Phase 4 shoshonitic lavas are more evolved than those in the latter stages of Phase 2 magmatism (see below), implying more opportunity for pooling, cooling and fractionation, this suggests that Phase 3 was associated with a tectonic event that led to significant crustal thickening in the Macquarie Arc.

PHASE 4 MAGMATISM

Phase 4 post-Eastonian uplift, post-Phase 3 magmatism in the Macquarie Arc was dominantly shoshonitic, with important representatives being the Wombin Volcanics, Northparkes Intrusives, Forest Reefs Volcanics, Millthorpe Volcanics and associated intrusive rocks around Cadia, Cheesemans Creek Formation, Malachis Hill Formation, Angullong Formation, Burranah Formation and much of the Sofala Volcanics. Compared with those shoshonites erupted immediately preceding the Eastonian uplift and Phase 3 magmatism, the Phase 4 magmatic units all contain a significantly larger volume of more evolved lavas, with basaltic lavas clearly subordinate to trachyandesitic–trachytic lavas, suggesting that these magmas had to pass through a thicker crust to allow more cooling and fractionation than that experienced by similar magmas erupted before the Eastonian hiatus. The post-Eastonian shoshonites show systematically lower initial ε_{Nd} values than those erupted earlier (Figure 14b) (Wyborn & Sun 1993), perhaps supporting more crustal interaction prior to eruption for these magmas. The Cu–Au-bearing porphyries at Northparkes and at least some of those at Cadia are final manifestations of the Phase 4 shoshonitic magmatism in the Macquarie Arc.

The Lower Silurian Nash Hill Volcanics, the magmas parental to the Fifield complexes, and rare small intrusive plugs (such as that intruding the Parkes Volcanics in a thrust slice adjacent to the Nash Hill Volcanics east of the Parkes Thrust, and also the Mt Olive monzodiorite in the Cadia district of the Molong Volcanic Belt) all show a distinctive compositional trend towards higher Nb than other Macquarie Arc lavas and intrusions. The petrogenetic scenario favoured for the Nash Hill Volcanics is that they represent the fractionation products of a basaltic parent magma produced by mixing of a shoshonitic basalt with an intraplate alkaline basaltic magma. The latter was significantly higher in LREE, Th, and U compared to the average intraplate basalt to account for the notably elevated contents of these elements in the Nash Hill Volcanics, and may even have approached a lamprophyric composition. As the Nash Hill Volcanics were deposited above or interfingering with the Llandoverian detrital quartz-rich part of the Cotton Formation, and the Fifield complexes were emplaced through and into recently folded quartz-rich flysch of the Girilambone Group, they may be better considered as a separate magmatic event, unrelated to the recently 'dead' Macquarie Arc.

ACKNOWLEDGEMENTS

We acknowledge receipt of an ARC SPIRT Grant that supported this work, with sponsorship and significant input from Alkane (Rob Chadwick, Ian Chalmers, Rimas Geraitas), Hargraves Resources (Damon Bird, Stuart Matthews), Homestake (Glen Twomey, Leigh Bettanay, Dave Mason), North Ltd (Stuart Smith, Mark Arundell), Newcrest (John Holliday, Ian Tedder, Mitch Bland), Goldfields Ltd (Bruce Mowat), and Resolute (Piers Reynolds). Dick Glen and Ian Percival (Geological Survey of New South Wales) contributed significantly to this project, and Peter Hollings, Carol Simpson and Rob Scott helped with fieldwork, sampling and discussions. We also thank University of Tasmania BSc (Hons) students Peter Duerden, Scott Boulton, Ami Libbiter and Rob Williams for their contributions to this project. Phil Blevin and Robin Offler are thanked for their useful reviews of the paper.

REFERENCES

AGNEW P. D. 1987. The petrology and geochemistry of the Tout and Owendale Complexes, Fifield, NSW. BSc (Hons) thesis, University of New South Wales, Sydney (unpubl.).

ANDREW A. S., HENSEN B. J., DUNLOP A. C. & AGNEW P. D. 1995. Oxygen and hydrogen isotope evidence for the origin of platinum-group element mineralization in Alaskan-type intrusions at Fifield, Australia. *Economic Geology* **90**, 1831–1840.

BARRON L. M. 1988. Platinum Project: petrology and chemistry of rocks. *Geological Survey of New South Wales Report* **GS1987/298** (unpubl.).

BARRON L. M. 2001. Petrology of Alaskan complexes in the Fifield platinum province, NSW. *In*: Crawford A. J., Glen R. A. & Cooke D. R. eds. *Final Report: SPIRT Ordovician Project*, pp. 5–75–5–90 (unpubl.).

BARRON L. M. & BARRON B. J. 1996. The limburgite suite in the Bathurst Dubbo area. *Geological Survey of New South Wales Quarterly Notes* **99**, 1–23.

BARRON L. M., SUPPEL D. W., SLANSKY E., JOHAN Z., OHNENSTETTER M. & SPENCER R. 1991. The Fifield Platinum Province. tectonics and metallogenesis of the Lachlan Fold Belt. *Geological Society of Australia Abstracts* **29**, 3.

BLEVIN P. L. 2002. The petrographic and compositional character of variably K-enriched magmatic suites associated with Ordovician porphyry Cu–Au mineralisation in the Lachlan Fold Belt, Australia. *Mineralium Deposita* **37**, 87–99.

BOULTON S. 2001. The Oakdale Formation in the Molong Belt, central west New South Wales. BSc (Hons) thesis, University of Tasmania, Hobart (unpubl.).

BOYNTON W. V. 1984. Geochemistry of the rare earth elements: meteorite studies. *In*: Henderson P. ed. *Rare Earth Element Geochemistry*, pp. 63–114. Elsevier, Amsterdam.

BUTERA K. M., WILLIAMS I. S., BLEVIN P. L. & SIMPSON C. J. 2001. Zircon U–Pb dating of Early Palaeozoic monzonitic intrusives from the Goonumbla area, New South Wales. *Australian Journal of Earth Sciences* **48**, 457–464.

CARR P. F., FERGUSSON C. L., PEMBERTON J. W., COLQUHOUN G., MURRAY S. I. & WATKINS J. J. 2003. Late Ordovician island-arc volcanic rocks, northern Capertee Zone, Lachlan Fold Belt, New South Wales. *Australian Journal of Earth Sciences* **50**, 319–330.

CLARKE I. 1990. Igneous Petrology. *In*: Clarke I. & Sherwin L. eds. *Geological Setting of Gold and Copper Deposits in the Parkes Area, NSW*, pp. 95–136. Geological Survey of New South Wales Record **23**.

COOKE D. R., WILSON A. J., HOUSE M. J., WOLFE R. C., WALSHE J. L., LICKFOLD V. & CRAWFORD A. J. 2007. Alkalic porphyry Au–Cu and associated mineral deposits of the Ordovician to Early Silurian Macquarie Arc, New South Wales. *Australian Journal of Earth Sciences* **54**, 445–463.

CRAWFORD A. J., COOKE D. R. & FANNING C. M. 2007. Geochemistry and age of magmatic rocks in the unexposed Narromine, Cowal and Fairholme Igneous Complexes in the Ordovician Macquarie Arc, New South Wales. *Australian Journal of Earth Sciences* **54**, 243–271.

DIREEN N. G., LYONS P., KORSCH R. J. & GLEN R. A. 2001. Integrated geophysical appraisal of crustal architecture in the eastern Lachlan Orogen. *Exploration Geophysics* **32**, 252–262.

Downloaded by [Auckland University of Technology] at 15:24 09 March 2015

Downloaded by [Auckland University of Technology] at 15:24 09 March 2015

DUERDEN P. B. 1999. Lithostratigraphy and lithogeochemistry of Ordovician volcano-plutonic rock in the Blayney area, central Molong Belt, NSW. BSc (Hons) thesis, University of Tasmania, Hobart (unpubl.).

ELLIOTT S. J. & MARTIN A. R. 1991a. Alaskan type intrusive complexes of the Fifield Belt, Central NSW. *In*: Elliott S. J. & Martin A. R. eds. *Geology and Mineralisation of the Fifield Platinum Province, New South Wales*, pp. 4–11. Sixth International Platinum Symposium, Guidebook for the Pre-symposium Field Excursion, Geological Society of Australia.

ELLIOTT S. J. & MARTIN A. R. 1991b. The Owendale Alaskan-type intrusive complex and associated PGE mineralisation, Fifield Belt, NSW. *In*: Elliott S. J. & Martin A. R. eds. *Geology and Mineralisation of the Fifield Platinum Province, New South Wales: 6th International Platinum Symposium, Guidebook for the Pre-symposium Field Excursion*, pp. 12–23. Geological Society of Australia, New South Wales Division, Sydney.

FALLOON T. J. 2001. The nature and affinities of the parental magma to the ultramafic series of the Late Ordovician Owendale intrusive complex, Fifield, central NSW. *In*: Crawford A. J., Glen R. A. & Cooke D. R. eds. *Final Report: SPIRT Ordovician Project*, pp. 5.35–5.58 (unpubl.).

GILL J. E. & WHELAN J. 1989. Early rifting of an oceanic arc (Fiji) produced shoshonitic to tholeiitic basalts. *Journal of Geophysical Research* **94**, 4561–4578.

GLEN R. A., CRAWFORD A. J., COOKE D. R. & PERCIVAL I. G. 2004a. Plate tectonics of the Lachlan Orogen: a framework for understanding its metallogenesis. *In*: Bierlein F. P. & Hough M. A. eds. *Tectonics to Mineral Discovery—Deconstructing the Lachlan Orogen*, pp. 33–36. Geological Society of Australia Abstracts **74**.

GLEN R. A., CRAWFORD A. J., PERCIVAL I. G. & BARRON L. M. 2007a. Early Ordovician development of the Macquarie Arc, Lachlan Orogen, New South Wales. *Australian Journal of Earth Sciences* **54**, 167–179.

GLEN R. A., MEFFRE S. & SCOTT R. J. 2007b. Benambran Orogeny in the Eastern Lachlan Orogen, Australia. *Australian Journal of Earth Sciences* **54**, 385–415.

GLEN R. A., SPENCER R., WILLMORE A., DAVID V. & SCOTT R. J. 2007c. Junee–Narromine Volcanic Belt, Macquarie Arc, Lachlan Orogen, New South Wales: components and structure. *Australian Journal of Earth Sciences* **54**, 215–241.

GLEN R. A., WALSHE J. L., BARRON L. M. & WATKINS J. J. 1998. Ordovician convergent-margin volcanism and tectonism in the Lachlan sector of east Gondwana. *Geology* **26**, 751–754.

GLEN R. A. & WATKINS J. J. 1999. Implications of Middle Devonian deformation of the eastern part of the Hill End Trough, Lachlan Orogen. *Australian Journal of Earth Sciences* **46**, 35–52.

GLEN R. A., ZHANG W., DAWSON M. & NEEDHAM J. 2004b. *Eastern Lachlan GIS*. Geological Survey of New South Wales, Sydney.

HOLLIDAY J. R., WILSON A. J., BLEVIN P. L., TEDDER I. J., DUNHAM P. D. & PRITZNER M. 2002. Porphyry gold–copper mineralisation in the Cadia district, eastern Lachlan Fold Belt, New South Wales, and its relationship to shoshonitic magmatism. *Mineralium Deposita* **37**, 100–116.

KAMENETSKY V. S., SOBOLEV A. V., JORON J-L. & SEMET M. P. 1995. Petrology and geochemistry of Cretaceous volcanics from Kamchatka. *Journal of Petrology* **36**, 637–662.

KRYNEN J. P., SHERWIN L. & CLARKE I. 1990. Stratigraphy and structure. *In*: Clarke I. & Sherwin L. eds. *Geological Setting of Gold and Copper Deposits in the Parkes Area, New South Wales*, pp. 3–76. Geological Survey of New South Wales Record **23**.

LICKFOLD V., COOKE D. R, CRAWFORD A. J. & FANNING C. M. 2007. Shoshonitic magmatism and formation of the Northparkes porphyry Cu–Au deposits, New South Wales. *Australian Journal of Earth Sciences* **54**, 417–444.

LICKFOLD V., COOKE D. R., SMITH S. G. & ULLRICH T. D. 2003. Endeavour copper–gold porphyry deposits, Northparkes, New South Wales: intrusive history and fluid evolution. *Economic Geology* **98**, 1607–1636.

LYONS P., RAYMOND O. L. & DUGGAN M. B. 2000. *Forbes 1:250 000 geological Sheet SI55-7, 2nd edition, Explanatory Notes*. Australian Geological Survey Organisation Record **2000/20**.

LYONS P. & WALLACE D. 1999. Geology and metallogenesis of the Parkes–Grenfell–Wyalong–Condobolin Region, New South Wales. *Australian Geological Survey Organisation Record* **1999/20**.

MEAKIN N. S. & MORGAN E. J. 1999. *Dubbo 1:250 000 Geological Sheet SI-55-4, 2nd Edition. Explanatory Notes*. Geological Survey of New South Wales, Sydney.

MEFFRE S., SCOTT R. J., GLEN R. A. & SQUIRE R. J. 2007. Re-evaluation of contact relationships between Ordovician volcanic belts and the quartz-rich turbidites of the Lachlan Orogen. *Australian Journal of Earth Sciences* **54**, 363–383.

MILES I. N. & BROOKER M. R. 1998. Endeavour 42 deposit, Lake Cowal, New South Wales: a structurally controlled gold deposit. *Australian Journal of Earth Sciences* **45**, 837–847.

MORGAN E. J., CAMERON R. G., COLQUHOUN G. P., MEAKIN N. S., RAYMOND O. L., SCOTT M. M., WATKINS J. J., BARRON L. M., HENDERSON G. A. M., KRYNEN J. P., POGSON D. J., WARREN A. Y. E., WYBORN D., YOO E. K. & GLEN R. A. 1999. *Dubbo 1:250 000 Geological Sheet SI/55-4* (2nd edition). Geological Survey of New South Wales, Sydney and Australian Geological Survey Organisation, Canberra.

MÜLLER D. & GROVES D. I. 2000. *Potassic Igneous Rocks and Associated Gold–Copper Mineralisation*. Springer, Berlin.

MÜLLER D., HEITHERSAY P. S. & GROVES D. I. 1994. The shoshonite porphyry Cu–Au association in the Goonumbla district, N. S. W., Australia. *Mineralogy and Petrology* **51**, 299–321.

MURRAY S. I. & STEWART I. R. 2000. Palaeogeographic significance of Ordovician conodonts from the Lachlan Fold Belt, southeastern Australia. *Historical Biology* **15**, 145–170.

OWEN M. & WYBORN D. 1979. Geology and geochemistry of the Tantangara and Brindabella 1:100 000 sheet areas, New South Wales and Australian Capital Territory. *Bureau of Mineral Resources Bulletin* **204**.

PACKHAM G. H., PERCIVAL I. G. & BISCHOFF G. C. O. 1999. Age constraints on strata enclosing the Cadia and Junction Reefs ore deposits of central New South Wales, and tectonic implications. *Quarterly Notes of the Geological Survey of New South Wales* **110**, 1–12.

PACKHAM G. H., KEENE J. B. & BARRON L. M. 2003.Middle to early Late Ordovician hydrothermal veining in the Molong Volcanic Belt, northeast Lachlan Fold Belt: sedimentological evidence. *Australian Journal of Earth Sciences* **50**, 257–269.

PERCIVAL I. G. 1999. Late Ordovician biostratigraphy of the northern Rockley–Gulgong Volcanic Belt. *Geological Survey of New South Wales Quarterly Notes* **108**, 1–7.

PERCIVAL I. G. 2000. Northparkes Volcanic Group. *In*: Lyons P., Raymond O. L. & Duggan M. B. eds. *Forbes 1:250 000 Geological Sheet SI55-7 (2nd edition), Explanatory Notes*, pp. 19–21. Australian Geological Survey Organisation Record **2000/20**.

PERCIVAL I. G. & GLEN R. A. 2007. Ordovician to earliest Silurian history of the Macquarie Arc, Lachlan Orogen, New South Wales. *Australian Journal of Earth Sciences* **54**, 143–165.

PERCIVAL I. G., MORGAN E. J. & SCOTT M. M. 1999. Ordovician stratigraphy of the northern Molong Volcanic Belt: new facts and figures. *Geological Survey of New South Wales Quarterly Notes* **108**, 8–27.

PERKINS C., MCDOUGALL I., CLAOUÉ-LONG J. & HEITHERSAY P. S. 1990. $^{40}Ar/^{39}Ar$ and U–Pb geochronology of the Goonumbla porphyry Cu–Au deposits New South Wales, Australia. *Economic Geology* **85**, 1808–1824.

PERKINS C., MCDOUGALL I. & WALSHE J. 1992. Timing of shoshonitic magmatism and gold mineralisation, Sheahan-Grants and Glendale, New South Wales. *Australian Journal of Earth Sciences* **39**, 99–110.

PERKINS C., WALSHE J. L. & MORRISON G. 1995. Metallogenic episodes of the Tasman Fold Belt system, eastern Australia. *Economic Geology* **90**, 1443–1466.

POGSON D. J. & WATKINS J. J. 1998. *Bathurst 1:250 000 Geological Sheet SI/55-8, 2nd Edition, Explanatory Notes*. Geological Survey of New South Wales, Sydney.

RAYMOND O. L., POGSON D. J., WYBORN D., HENDERSON G. A. M., KRYNEN J., MEAKIN S., MORGAN E. J., SCOTT M. M., STUART-SMITH P., WALLACE D., WARREN A. Y. E., WATKINS J. J. & GLEN R. A. 1998. *Bathurst 1:250 000 Geological Sheet SI/55-8*. Geological Survey of New South Wales, Sydney and Australian Geological Survey Organisation, Canberra.

RAYMOND O. L. &. SHERWIN L. 1999. *Geology of the Parkes 1:100 000 Geological Sheet 8531, Preliminary Edition*. Australian Geological Survey Organisation, Canberra, and Geological Survey of New South Wales, Sydney.

ROGERS N. W. & SETTERFIELD T. N. 1994. Potassium and incompatible-element enrichment in shoshonitic lavas from the Tavua volcano, Fiji. *Chemical Geology* **118**, 43–62.

SCOTT M. M., MORGAN E. J. & POGSON D. J. 1998. Cheesemans Creek Formation. *In*: Pogson D. J. & Watkins J. J. eds. *Bathurst 1:250 000 Geological Sheet SI/55-8, Explanatory Notes*, pp. 68–70. Geological Survey of New South Wales, Sydney.

SHERWIN L. 1996. *Narromine 1:250,000 geological Sheet SI/55-3, Explanatory Notes.* Geological Survey of New South Wales, Sydney.

SIMPSON C. J., CAS R. A. F. & ARUNDELL M. C. 2005. Volcanic evolution of a long-lived Ordovician island-arc province in the Parkes region of the Lachlan Fold Belt, southeastern Australia. *Australian Journal of Earth Sciences* **52**, 863–886.

SIMPSON C. J., SCOTT R. J., CRAWFORD A. J. & MEFFRE S. 2007. Volcanology, geochemistry and structure of the Ordovician Cargo Volcanics in the Cargo-Walli region, central New South Wales. *Australian Journal of Earth Sciences* **54**, 315–352.

SPENCER R. 1990. Interpretation of regional and detailed aeromagnetic data over the Owendale Intrusive Complex, Fifield, New South Wales. *Geological Survey of New South Wales Quarterly Notes* **80**, 19–37.

SPROULE R., LAMBERT D. D. & MURPHY D. 1996. Re–Os and Sm–Nd isotopic and geochemical constraints on the source of the Owendale Alaskan type complex, Fifield, NSW. *Geological Society of Australia Abstracts* **41**, 415.

SQUIRE R. J. & CRAWFORD A. J. 2007. Magmatic characteristics and geochronology of Ordovician igneous rocks from the Cadia–Neville region, New South Wales: implications for tectonic evolution. *Australian Journal of Earth Sciences* **54**, 293–314.

SQUIRE R. J. & MCPHIE J. 2007. Complex volcanic facies architecture of the Forest Reefs Volcanics near Cadia, New South Wales, associated with prolonged arc–related volcanism. *Australian Journal of Earth Sciences* **54**, 273–292.

STOJANOVIC M. 1995. Petrology, geochemistry and isotope geochemistry of host rocks to platinum mineralisation at Fifield, New South Wales. MSc thesis, University of New South Wales, Sydney (unpubl.).

SUN S-S. & MCDONOUGH W. F. 1989. Chemical and isotopic systematics of oceanic basalts: implications for mantle composition and processes. *In*: Saunders A. D. & Norry M. J. eds. *Magmatism in the Ocean Basins*, pp. 313–345. Geological Society of London Special Publication **42**.

TAYLOR S. R. & MCLENNAN S. M. 1985. *The Continental Crust: Its Composition and Evolution.* Blackwell, Oxford.

VERBEETEN A. C. 1996. Petrology, geochemistry and tectonic implications of magmatism along the northern Hunter Ridge and on Kadavu Island Group, Fiji. PhD thesis, University of Tasmania, Hobart (unpubl.).

WATKINS J. J. 1996. Regional setting of structurally hosted gold mineralisation in the Mudgee–Gulgong district NSW. MEconGeol thesis, University of Tasmania, Hobart (unpubl.).

WATKINS J. J. 1998. Sofala Volcanics. *In*: Pogson D. J. & Watkins J. J. eds. *Bathurst 1:250 000 Geological Sheet SI/55-8, Explanatory Notes*, pp. 74–76. Geological Survey of New South Wales, Sydney.

WATKINS J. J. 1999. Burranah Formation. *In*: Meakin N. S. & Morgan E. J. eds. *Dubbo 1:250 000 Geological Sheet SI/55-4, Explanatory Notes*, pp. 41–44. Geological Survey of New South Wales, Sydney.

WILLIAMS R. 1999. Geology and geochemistry of the Byng Volcanics, east of Orange. BSc (Hons) thesis, University of Tasmania, Hobart (unpubl.).

WYBORN D. 1992. The tectonic significance of Ordovician magmatism in the eastern Lachlan Fold Belt. *Tectonophysics* **214**, 177–192.

WYBORN D. & HENDERSON G. A. M. 1996. *Explanatory Notes: Blayney 1:100 000 Geological Sheet.* Australian Geological Survey Organisation, Canberra.

WYBORN D., OWEN M. & WYBORN L. 1990. *Geology of the Kosciusko National Park (1:250 000 scale map).* Bureau of Mineral Resources, Canberra.

WYBORN D. & SUN S-S. 1993. Nd-isotopic 'fingerprinting' of Cu/Au mineralisation in the Lachlan Fold Belt. *AGSO Research Newsletter* **19**, 13–14.

XUE Y-Y. 1990. The petrology and geochemistry of the Tout Complex. *Geological Survey of New South Wales Report* (unpubl.).

Received 16 April 2006; accepted 12 January 2007

Downloaded by [Auckland University of Technology] at 15:24 09 March 2015

APPENDIX 1: LOCATION (AMG) AND PETROGRAPHY OF ANALYSED SAMPLES IN TABLE 1

Sample no.	Rock type	Easting	Northing
Goonumbla Volcanics Basal Mafic Unit			
CSG112	Pl+cpx+sp ol+FeTiox-phyric basalt, 2 opaques	599557	6343748
CSG23	Pl+cpx+sp ol+FeTiox-phyric basalt, fresh plag and cpx	603877	6349455
CSG88	Pl+cpx+sp ol+FeTiox-phyric basalt	601301	6346654
Goonumbla Volcanics			
10-22-1	Plag+cpx+ap+FeTiox-phyric andesite	605354	6340198
CSG100	Plag+biotite+sp cpx+ap+FeTiox-phyric andesite	597095	6346645
CSG89	Plag+cpx+ap+FeTiox-phyric andesite	601154	6345423
CSG141B	Plag+cpx+ap+FeTiox-phyric andesite	596474	6340820
Wombin Volcanics			
CSG12	Plag+biotite+hbd+sp cpx+ap+FeTiox-phyric andesite	601842	6352582
CSG107	Plag+sp cpx+ap+FeTiox-phyric andesite	597489	6347495
10-22-12	Plag+biotite+ap+FeTiox-phyric dacite	607010	6342181
Post-Mineralisation E37 'Zero' Trachyte dykes			
E37H3-245.2	Biotite+pl+apatite+Kspar-phyric trachyte	592493	6357110
Parkes Volcanics			
BV5	Mod. plag-phyric cpx-poor andesite	607215	6332720
BV7	Foliated plag-phyric andesite	607205	6332725
BV8	Mod. plag-phyric cpx-poor andesite dyke	607245	6332735
BV6	Plag+Kspar+qtz-phyric microgranodiorite	607205	6332725

(*continued*)

APPENDIX 1 (*Continued*).

Sample no.	Rock type	Easting	Northing
Bushman Volcanics			
W1288A	Sl. chlorite-altd cpx-phyric basaltic lava bx	610200	6333900
10-18-1	Strongly plag+cpx+FeTiox-phyric andesite	620820	6345110
BV1	Sl autobx hbd+pl+sp cpx+ap-phyric andesite	610150	6333950
BV3	Hbd+plag-phyric lv bx	610150	6333950
Nash Hill Volcanics			
NH19	Strongly cpx-phyric bas with occ ol+pl phens	611280	6335400
NH15	Pl+hbd+apatite+FeTiox-phyric andesite	611008	6336010
NH18	Finely plag+cpx+hbd+FeTiox-phyric andesite	611200	6335430
NH21	Finely pl+cpx+hbd+FeTiox-phyric basalt	611505	6335180
Northparkes Igneous Complex Intrusions (regional)			
CGS11	Monzodiorite with biotite, fresh cpx, lots of apatite	602010	6352582
CSG59B	Quite coarse monzodiorite; fresh cpx with melt incl.	604351	6348063
CSG189	Monzonite	595201	6344786
E28H13-53.8	Altd biotite monzonite	598407	6354978
Lower Blayney Volcanics			
MB98	Gschist facies mod cpx-phyric basaltic lava	699840	6288830
PBD36	Cpx-phyric basalt, sparse altered ol phenos & plag mphens	702955	6290357
PBD52	Cpx-phyric basalt, sparse altered ol phenos & plag mphens	703623	6291796
PBD157	Cpx-phyric basalt	703265	6291446
Upper Blayney Volcanics			
MB3	Cpx+plag+sp ol-phyric basalt with v fine-gr gmass	700700	6288750
RSMB5	Coarsely cpx+ol-phyric glassy lava. Nearly umafic	703599	6303750
MB12	Low gschist facies ankaramite	717300	6275545
MB80	V dark fine-gr v sparsely ol+cpx-phyric basalt	704295	6302801
Millthorpe Volcanics			
PBD21	Cpx+plag-phyric basalt, rare ol phenos	702431	6292050
PBD39	Cpx+plag-phyric basalt, rare ol phenos	704176	6293974
PBD42	Cpx+plag-phyric basalt, rare ol phenos	703997	6294036
PBD56	Cpx+plag-phyric basalt, rare ol phenos	698964	6291527
Byng Volcanics			
RDW170	Basalt	707610	6305490
RDW193	Coarsely cpx+ol-phyric glassy lava; some plag mphens	707450	6307770
RDW80	Coarsely strongly cpx-phyric ankaramite, fresh cpx	710612	6301850
RDW142	Coarsely strongly cpx-phyric ankaramite, fresh cpx	709008	6303380
RDW119	Umafic lava, abundant large ol, int cpx and minor phlogopite	709902	6307856
RDW178	Umafic lava, abundant large ol, int cpx and minor phlogopite	708780	6305600
RDW140	Umafic lava, abundant large ol, int cpx and minor phlogopite	709005	6302950
Coombing Fmn dykes			
BLRS0139	Dolerite	694980	6265810
BLRS0189	Dolerite	697850	6273980
Cheesemans Creek Formation			
KA80	Sl altd plag+cpx-phyric basalt,	677900	6324300
OR8	V plag-rich basalt, chlor-altd cpx and ol, elongate gmass FeTiox	677775	6324407
KA33	Strongly coarsely pl-phyric basalt, occ fresh cpx, big FeTiox	674470	6336000
KA78	Big plag basalt, sparse cpx, small apatite mphens	677700	6323560
Angullong Formation			
WA27	Finely plag+cpx+occ olive hbd-phyric basaltic andesite	678417	6284280
WA15	Hbd+cpx+plag+ap-phyric andesite shallow intrusive	676334	6285185
Fairbridge Volcanics (Units 1–3 southern section)			
KA38a	Strongly cpx-phyric basalt, some altd ol, some plag mphens	678400	6333200
OR12	Coarsely cpx-phyric basalt, occ altd ol, plag mphens common	674177	6347005
OR61	Cpx-rich basalt with minor plag, fine gmass	677211	6334175
OR95	Cpx-phyric basalt, subord altd ol and some plag mphens	677180	6333363
Fairbridge Volcanics (Units 4–6 southern section)			
OR99	Vesic plag-rich basalt with CO3-altd cpx+ol phenos	676211	6333180
KA60	Big plag+cpx-phyric basalt lava	674200	6348220
OR98	Abundantly plag-phyric basalt, common CO3-altd ol and big cpx	676274	6333302
OR109	Strongly plag-phyric basalt, occ altd cpx, big apatites	676314	6335568

(*continued*)

Downloaded by [Auckland University of Technology] at 15:24 09 March 2015

APPENDIX 1 (*Continued*).

Sample no.	Rock type	Easting	Northing
Fairbridge Volcanics (Units 1–3 northern section)			
MB403	Sl altd cpx+plag-phyric andesite, occ apatites	676500	6376500
KA31	Strongly ol+cpx-phyric basalt, big oxides, altd ol, some fresh cpx	676230	6358920
KA24	Vesci plag+cpx+altd ol-phyric basalt, some small chromites	675220	6358550
KA49	Strongly cpx+plag-phyric pillow basalt, small altd ols	674500	6354360
Transitional alkaline dykes			
RS8–9	Ti-augite-bearing alkali dolerite dyke, Cargo block	671600	6309800
OR46	Aphyric dol with clear cpx but elongate FeTioxides	681403	6332342
MB364	Ti-augite+ilmenite bearing aphyric dolerite	680220	6380220

Downloaded by [Auckland University of Technology] at 15:24 09 March 2015

APPENDIX 2: MILLTHORPE VOLCANICS

Name After the village of Millthorpe on the New South Wales 1:100 000 Map Sheet 8731 and the Bathurst 1:250 000 map sheet.

Synonymy Formerly mapped as the southwestern part of the Byng Volcanics by Pogson and Watkins (1998), but the Millthorpe Volcanics are significantly more evolved than the primitive olivine-phyric Byng Volcanics.

Distribution and type locality In a broad and generally poorly outcropping area centred on 33°29.5'S, 149°10'E (between 701000 and 702500E, and 629800 and 6295000N: UTM Zone 55 GDA94), in the region north-northeast of Browns Creek mine, including the middle reaches of Limestone Creek, which is considered to be the type locality.

Stratigraphic relationships West of Browns Creek mine, there is a passage upward from the upper Blayney Volcanics into the more evolved, plagioclase-phyric lavas of the Millthorpe Volcanics. At several locations the Millthorpe Volcanics occur above the poorly dated Upper Ordovician Cowriga Limestone Member, although the nature of the contact is unclear.

Thickness At least 500 m, possibly as much as 900 m

Lithology Plagioclase + clinopyroxene-phyric evolved shoshonitic basalt and basaltic andesite lavas with subordinate volcaniclastic sandstones. Occasional clinopyroxene + hornblende-phyric basaltic andesite lavas.

Age Late Ordovician, probably late Eastonian to Bolinidan based on age of the Cowriga Limestone in the immediately underlying upper Blayney Volcanics.